PROCESS OPTIMIZATION FOR AN INTEGRATED REVERSE OSMOSIS—PRESSURE RETARDED OSMOSIS PILOT-SCALE SYSTEM OPERATED ON HUMBOLDT BAY, CA

By

Galen O'Toole

A Thesis Presented to

The Faculty of California State Polytechnic University, Humboldt

In Partial Fulfillment of the Requirements for the Degree

Master of Science in Environmental Systems: Environmental Resources Engineering

Committee Membership

Dr. Margaret Lang, Committee Chair

Dr. Andrea Achilli, Committee Member

Dr. Tesfayohanes Yacob, Committee Member

Dr. Margaret Lang, Program Graduate Coordinator

December 2022

ABSTRACT

PROCESS OPTIMIZATION FOR AN INTEGRATED REVERSE OSMOSIS—PRESSURE RETARDED OSMOSIS PILOT SYSTEM OPERATED ON HUMBOLDT BAY, CA

Galen O'Toole

Pressure retarded osmosis (PRO) is an emerging osmotic power technology that could mitigate the major challenges faced by seawater reverse osmosis desalination (RO): brine disposal and high energy consumption. The primary focus of this paper is process optimization for a linked seawater reverse osmosis (RO) and pressure retarded osmosis (PRO) water purification system. PRO generates power by using osmosis to "pump" water through a membrane from low pressure and low concentration to high pressure and high concentration (RO brine). This commercial-scale pilot effort explores process optimization for pressure retarded osmosis as an industrial process rather than theoretical or experimental process. To achieve this purpose, a linked seawater desalination and pressure-retarded osmosis system was built on Humboldt Bay, CA, with assistance from Cal Poly Humboldt, CA DWR, and the Humboldt Bay Harbor Commission.

This study explored the lowest net specific energy consumption (SEC_{net}) for producing freshwater from seawater in the first U.S. RO-PRO pilot-scale facility employing commercially-available components. The lowest SEC_{net} was found by adjusting and testing six operating variables: RO yield rate, PRO operating pressure, PRO dilution rate, PRO feed solution flow rate, and PRO draw solution flow rate. Each variable was tested independently to narrow the range of optimal values. Findings

conclude that energy losses in the RO-PRO system approximately equal the amount of potential energy that can be gained using PRO membranes available in 2017. Increasing membrane performance and optimizing module membrane spacers for PRO could significantly increase potential energy recovered by PRO in an RO-PRO system.

ACKNOWLEDGEMENTS

- Advisory committee: Dr. Andrea Achilli, Dr. Margaret Lang, Dr. Tesfayohanes Yacob
- HSU technicians: Colin Wingfield and Marty Reed, Louis McCrigler
- California Department of Water Resources
- Humboldt Bay Harbor District
- Prof. Amy Childress and Lauren Crawford at USC
- HSU undergraduates: Laurel Smith, Patrick Hassett, Kelsey Burrell, and Spencer McLintock
- Francesco Piana, visiting doctoral student from University of Bologna
- Dr. Mary Theresa Pendergast at Oasys Water

TABLE OF CONTENTS

LIST OF TABLES

LIST OF FIGURES

LIST OF APPENDICES

I. INTRODUCTION

Water is so necessary for life and human development that most of us take it for granted. As humans have spread across the planet and dug into the earth's crust for resources, we have begun to understand the finite quality of those resources (United Nations, 2015). Few people are willing to contemplate and address the growing scarcity of fresh, usable water. In the United States, water is expected to be delivered as a public good, yet the procurement of water is often challenging for many cities and public utilities as procurement is couched in the framework of private ownership, antiquated water rights law, and profit motives for water allocations. The inherent conflict between public and private access to water comes to the fore when water is scarce, as in California during frequent and recently increasing drought periods. The majority of water resources in California are privately owned, due to seniority of private water rights that stretch back to the mid-to-late 1800s. During drought times, private senior water rights holders have first priority for limited water resources—many municipalities are forced to pay higher prices and use marginal sources to keep taps flowing to homes and businesses. Groundwater was the second source to be developed after surface water, but it has been withdrawn much faster than it has been replenished, causing major reductions in availability and causing both subsidence and saltwater intrusion. Many coastal communities are attempting to solve their water resources deficit by installing reverse osmosis desalination facilities.

Reverse osmosis seawater desalination (RO) could provide an ever-present freshwater source for coastal communities around the world. However, three major drawbacks prevent widespread use of RO technology. First, RO requires high energy usage, contributing to monetary cost and significant greenhouse gas (GHG) emissions. Second, RO creates a concentrated saline brine that may harm local marine ecosystems when discharged to the ocean. Third, RO is a high-tech, expensive technology that often requires a public/private partnership for municipal water development (Authority, 2017). High energy usage and brine discharge from municipal RO can be mitigated through technological solutions, but equitable access to water can be at risk when water resources are privatized.

These three drawbacks for RO can be mitigated, but it is important to keep in mind that privatization of water resources creates an inherent conflict between private interests and the public good. The private sector generally seeks to maximize profits and has little incentive for distributing resources equitably. Water is a necessity of human life, and there is significant precedence set that it should be regarded as a public good (Institute, 2010). Private control of public water sources poses a risk to public water security, especially for disadvantaged communities.

Pressure retarded osmosis (PRO) is one potential technological solution to the energy and saline discharge drawbacks of seawater RO (Achilli et al. 2014). Energy can be gained by mixing RO brine with an impaired freshwater source, simultaneously diluting the brine before discharge and lowering the energy required for extracting freshwater (Achilli et al. 2014). The RO and PRO process details, thermodynamics and

the current state of membrane technology are elucidated in the main body of this study. A thermodynamic analysis of physical tests from the first fully-integrated RO-PRO system showed a significant potential for reducing energy required to produce freshwater from seawater compared to the current standard of RO technology (Achilli et al. 2014).

The primary focus of this paper is process optimization for a linked seawater reverse osmosis and pressure retarded osmosis water purification system. This commercial-scale pilot effort explores process optimization for pressure retarded osmosis as an industrial process rather than theoretical or experimental process. To achieve this purpose, a linked seawater desalination and pressure-retarded osmosis system was built on Humboldt Bay, CA, with assistance from Cal Poly Humboldt, CA DWR, and the Humboldt Bay Harbor Commission. Four goals helped to shape the pilot system and the objectives of the study:

1. Maximize and measure energy that can be recovered by PRO for producing freshwater from seawater when using commercially-available components in a linked RO-PRO system.
2. Evaluate the current commercial viability of pressure retarded osmosis on an industrial scale when coupled with seawater RO
3. Provide operational data tied to specific membranes that allows the reader to use this paper as a case study and to inform other pilot efforts.
4. Test the process using commercially available equipment in a configuration that could be considered a minimum modular size

A thermodynamics model was developed based on previous work (Achilli et al. 2009) and used to estimate and evaluate energy used by seawater RO, and energy recovered by a linked PRO sub-system. Modeling for an RO-PRO linked system formed the basis for designing, building, and operating a physical system to conduct pilot-scale process optimization of a seawater RO-PRO system. The modeling study was

accomplished in two parts: first PRO alone, then PRO in combination with seawater RO. A seawater RO-PRO pilot was built using commercially-available components and operated for several months taking seawater input from Humboldt Bay. Data was collected from running the pilot with operating parameters at various set-points to establish membrane functionality and estimate a best operating point (BOP). Overall system viability was evaluated by measuring energy recovery by PRO and energy losses in the pilot system when operated at the BOP.

II. LITERATURE REVIEW

Many research efforts have focused on seawater reverse osmosis desalination (RO), and pressure retarded osmosis (PRO). This literature review focuses on seminal works in PRO development and linked RO-PRO applications. These selected works have provided the fundamental conceptual and thermodynamic understanding necessary to develop RO-PRO from original concept to potential commercial viability.

1. Pressure retarded osmosis (PRO)

In 1975 PRO was first theorized to have the capacity to generate power from the potential energy between seawater and freshwater sources such as rivers near their discharge to the ocean (Loeb, 1975). PRO relies on osmosis through a semi-permeable membrane that separates a low-concentration (feed) solution from a high-concentration (draw) solution. Osmotic pressure, or potential energy, between two solutions increases as the salinity gradient between them increases. Work can be harnessed from osmotic pressure by pressurizing the draw solution to less than the osmotic pressure (π) so that water continues to pass through the membrane from the feed solution to the pressurized draw solution, see Figure 1. The osmotic pressure drives water from low pressure (feed) to high pressure (draw), and the increased flow in the draw solution can be diverted to perform work (Achilli et al. 2009). The remaining draw flow rate passes through an energy recovery device, such as a pressure exchanger, and transfers its potential energy to the incoming un-diluted draw flow (Figure 1).

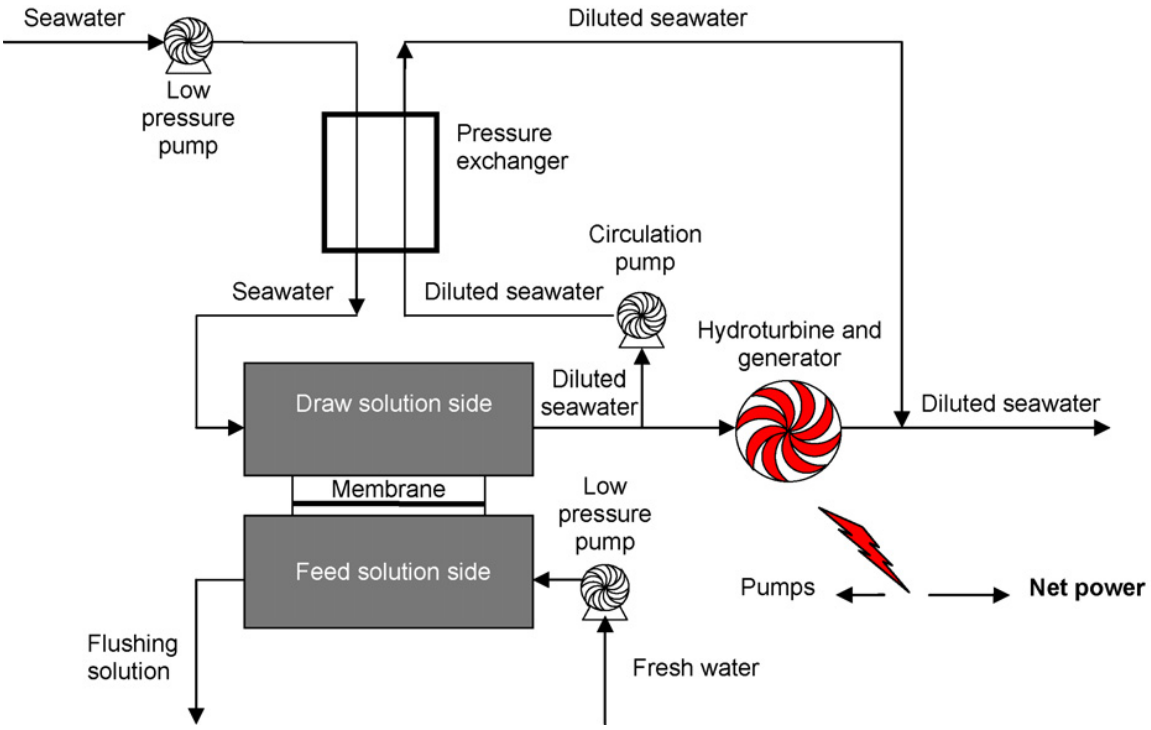

Figure 1: Theoretical pressure retarded osmosis (PRO) system. Water flows across the membrane from the feed solution (low pressure, low salinity) to the draw solution (high pressure, high salinity). The increase in draw solution flow rate, that is at an elevated pressure, can be harnessed for work. Figure from (Achilli et al. 2009)

The amount of power that can be generated from PRO is limited by the following:

1. difference in salinity between the two solutions (salinity gradient),
2. theoretical limits of the system process depicted in Figure 1,
3. energy losses in pumps, pipes, membranes, and energy recovery devices, and
4. practical operability of a physical system (the focus of this study)

Total work possible from PRO is represented by

Equation 1. $W = J_w * \Delta P$

Where W is work, J_w is the freshwater flux through the membrane, and ΔP is the difference in pressure between feed and draw solutions. Water flux (J_w) is a function of the membrane's water permeability coefficient and the difference between the osmotic pressure and physical pressure difference between the two solutions. Achilli and

colleagues demonstrate that maximum theoretical work is a function of the osmotic pressure and the membrane permeability coefficient (Achilli et al. 2009):

Equation 2. $W_{max} = A * \frac{\Delta\pi^2}{4}$

Power, as the derivative of work, yields a maximum point when $\Delta P = \frac{1}{2} \pi$ (Achilli et al. 2009).

The ½ π value is important as it yields maximum theoretical power, assuming ideal membrane characteristics. Previous work (O'Toole et al., 2016) focused on modeling and optimizing a design for a commercial-scale PRO facility, using non-ideal membrane parameters and friction losses in a theoretical PRO facility. A linked-simulation optimization (LSO) model was created to estimate maximum energy production by the PRO commercial facility combining river water with seawater. This first optimization modeling study was published in *Desalination* and was the motivation for this master's thesis (O'Toole et al., 2016). The final findings of this modeling effort were that the energy required by feed water pre-treatment and friction losses approximately equaled the energy that could be gained from combining freshwater and seawater with PRO. A greater salinity gradient would provide much more potential energy since pre-treatment and friction losses would be relatively constant, while increasing the salinity gradient would provide linearly increasing potential energy as the difference in salinity increases between PRO feed and draw solutions. A realistic source for a higher salinity draw solution could be the brine discharge from a seawater reverse osmosis facility (Achilli et al., 2014).

The most influential variables in optimizing PRO energy recovery are salinity gradient, transmembrane pressure (TMP), flow rates, and mass transport rates for salts and freshwater through the PRO membrane. TMP and the difference in salinity across the PRO membrane control mass transport rates, while flow rates control friction losses and have minimal impact on mass transport. The goal with any salt-exclusive membrane, Forward Osmosis (FO), RO, or PRO, is to minimize salt transport and maximize pure water transport through the membrane. Membrane defects and pressure-driven membrane deformation were known to significantly impact real world performance of forward osmosis (Company) membranes operated in PRO tests (Skilhagen, 2010).

Additional modeling efforts performed by Binger and Achilli used PRO performance to develop an RO-PRO model accounting for real-world energy consumption, process losses, and to compensate for membrane imperfections and operational deformations (Binger et al., 2021). This model was calibrated with test data of commercial FO membrane modules in the seawater RO-PRO pilot operated at Samoa, CA. The modeling was used to estimate a simple minimum of energy required to produce freshwater from a seawater RO-PRO combined system. This updated model was published in The Journal of Membrane Science in 2021 and fulfills the first three goals through a modeling approach: (1) explore energy recover of PRO in RO-PRO configuration, (2) evaluate commercial viability, (3) obtain data from commercially-available membranes to inform additional efforts (Binger et al., 2021).

2. Reverse osmosis desalination

Seawater RO desalination is the process of producing freshwater from seawater by forcing seawater through a semi-permeable membrane under high pressure. A seawater RO membrane is a very tough, thin, hydrophobic membrane that rejects salts while allowing pure water to pass through. In order to force water through the membrane, pressure must be applied that exceeds the osmotic pressure of the seawater. Pumping seawater to such high pressures (~700-900 psi) requires a lot of energy for every unit of freshwater produced. Specific energy consumption (SEC) of seawater RO is the primary metric used to evaluate cost of desalination—SEC is the amount of energy required to produce one unit volume of freshwater permeate, typically in units of kWh/m^3. Energy required for RO desalination has diminished considerably in recent years due to increased understanding of the thermodynamic process, isobaric energy recovery, and improved membranes and spacers. Membrane and spacer advancements have drastically lowered the amount of membrane area necessary for RO desalination and reduced the frictional losses through RO modules (Lee et al. 2011, Shenvi et al. 2015).

These advancements have been further improved by the addition of energy recovery devices (ERDs), such as isobaric pressure exchangers (PXs), which have increased in efficiency over the last 20 years and can now recover up to 98% of the pressure in the concentrate stream (Andrews and Laker 2001, Fritzmann et al. 2007), (Shumway 1999) & (Stover and Andrews 2012)). These new PX devices have reduced the SEC for RO by as much as 50% (Feinberg et al. 2013) to 60% (Stover and Andrews 2012).

Operational and design improvements have also benefitted from the understanding that for a single-stage RO process, the theoretical minimum SEC is at 50% RO recovery without ERDs, while the addition of ERDs causes the SEC to increase as RO recovery increases ((Zhu, et al. 2009) & (Prante et al. 2014). With current technology, the minimum theoretical SEC of a single-stage RO desalination facility operating at 50% RO recovery is 1.54 kWh/m^3 (Chong et al. 2015). Realistic RO systems could achieve SEC of 2.0 to 2.12 kWh/m^3 (Peñate and García-Rodríguez 2012, Shrivastava et al. 2015), respectively. The Ashkelon seawater desalination plant in Israel is one of the most efficient facilities currently in operation, and it consumes approximately 3.9 kWh/m^3 (Sauvet-Goichon 2007), but this higher number includes pretreatment and conveyance to a distribution network and storage.

3. RO-PRO

Osmotic energy reduction strategies in the RO process have been proposed by hybridizing RO with passive osmotic dilution (forward osmosis) (Cath et al. 2010) or osmotic energy recovery (pressure retarded osmosis, reverse electro dialysis) (Achilli et al. 2009, Saito et al. 2012, Feinberg et al. 2013, Y. Kim et al. 2013, and Prante et al. 2014). PRO has the thermodynamic potential of recovering approximately 50% of the chemical (osmotic) energy in the RO brine effluent (J. Kim et al. 2013, Sim et al. 2013). PRO can reduce the energy cost of RO desalination by recovering chemical potential energy from the RO brine stream by using osmosis to increase flow in a pressurized PRO

draw stream (coming from RO brine) and then transferring the pressure energy from the increased PRO draw flow to the pressurized RO feed.

From an entropy analysis, RO facilities decrease entropy, thereby increasing potential chemical energy between brine and fresh permeate water. This decrease in entropy is achieved by adding energy (pressure) to seawater and forcing freshwater through a membrane, increasing the salt concentration of the brine. The resulting permeate and brine from RO provides an increased salinity gradient that provides greater potential energy that can be harnessed to reduce the energy cost of RO desalination. PRO harnesses the difference in entropy between two solutions as potential energy by allowing water to pass through a semipermeable membrane from low salinity and low pressure to high salinity and high pressure. The potential energy harnessed by PRO is imparted to incoming RO feed seawater via an energy recovery device and thereby offset pumping costs for RO purification (Figure 2).

The analysis presented here focuses on pressure retarded osmosis (PRO) which harnesses work from the flux of water through a semipermeable membrane from a solution with low ionic concentration and low pressure to a solution with higher concentration and pressure (Loeb and Mehta 1979). The amount of work that can be harnessed increases as the difference in the ionic strength of the two solutions increases (Skilhagen et al. 2008), making PRO more attractive when designed for higher concentration brines. The work, normalized to a unit volume of permeate, is the specific energy (SE_{PRO}) (Yip and Elimelech 2012). SE_{PRO} is a function of the draw stream

dilution, the hydraulic pressure difference across the membrane, and the osmotic pressure difference ($\Delta\pi$) between the solutions (Yip and Elimelech 2012).

Equation 3. $W_{PRO} = \Delta P * \Delta V$ (kWh)

Equation 3 is the same as Equation 1, but ΔV is substituted for J_w as the volume of water passing through the membrane was directly measured in this study. Ideal work in the PRO process is represented by Equation 3, where ΔP is the hydraulic pressure difference across the membrane, and ΔV is the increase in volume of the draw solution due to water permeating through the membrane.

Equation 4. $SE_{PRO} = \frac{\Delta P * \Delta V}{V_p}$ (kWh/m^3)

The specific energy (SE_{PRO}) is the energy gained per unit volume of the limiting resource, freshwater. Freshwater permeating through the membrane which is represented by V_p in Equation 4.

PRO still faces several design challenges to achieve commercial viability: a lack of PRO-specific membranes (Han et al. 2015), little published research on module-scale physical tests ((Y. Kim et al. 2013), (Achilli et al. 2014), (Saito et al. 2012) & (Skilhagen, 2010)), high energy costs of pretreatment ((Saito et al. 2012), (Maisonneuve et al. 2015) & (D. Kim et al. 2015)), and virtually no long-term studies of fouling and cleaning protocols.

4. Energy reduction potential for seawater RO

The potential benefit of PRO to RO desalination is taken one step further by He and coworkers (2014) in their analysis of a proposed standalone RO-PRO facility. Ideal

conditions are assumed for the thermodynamic analysis of an RO-PRO facility, where the energy consumption comes from the high-pressure pump only. In the ideal case, where pretreatment costs are also ignored, they conclude that RO-PRO could be energy-positive if the diluted effluent from the PRO system is less concentrated than the seawater influent to the facility (He et al. 2014). However, large volumes of low-salinity water are generally scarce in locations employing desalination, and the energy cost of pretreatment is a significant factor ((Saito et al. 2012), (Altaee and Sharif 2015) & (D. Kim et al. 2015)).

The tradeoff between osmotic dilution and osmotic energy recovery is described by J. Kim and coworkers (2013): the efficiency of RO decreases and the efficiency of PRO increases with increasing brine concentration. Kim and coworkers define the water energy return rate (WERR) in order to compare the benefit gained from varying configurations and operating parameters for RO and PRO (J. Kim et al. 2013). They conclude that RO parameters dominate the WERR value, but PRO parameters can significantly reduce energy costs associated with RO.

The energy reduction potential of a PRO subsystem for RO is dependent on a number of factors including the ratios of seawater to low-salinity feed water to produced water (SW : FW : PW). This ratio is determined by the recovery, or yield, (Y) of the RO system and dilution in the PRO system. Prante et al. (2014) constructed an RO-PRO model and tested the SEC of producing RO permeate for three scenarios: RO, RO-PX, and RO-PRO. The model results for the RO-PX system showed a minimum SEC of 1.45 kWh/m^3 at 13% recovery, increasing to 2.00 kWh/m^3 at 50% recovery (Prante et al.

2014). For the RO-PRO (with PX) system the SE_{PRO} increased with increasing dilution, and higher dilutions were possible at higher recoveries (Prante et al. 2014). However, the total SEC was more sensitive to changes in RO recovery than changes in PRO dilution; the lowest SEC was reported for 30% RO recovery and a maximum of 50% dilution. The modeled SEC for RO with PRO and energy recovery devices was approximately 1.25 kWh/m^3 for 40% RO recovery and 40% PRO dilution (Prante et al. 2014). The same modeled system was tested with a module-scale pilot project by Achilli and colleagues (2014), where RO recoveries were 20% and 30%, and the RO-PRO system employed one pressure exchanger for the PRO module effluent. Using synthetic seawater (33-35 g/L NaCl) and tap feed water, results showed no reduction in SEC for the RO-PRO system because of pressure lost between the RO and PRO subsystems (Achilli et al. 2014). If a second pressure exchanger were present to capture the lost pressure, the SEC for the RO-PRO system would be 22% lower than the SEC for RO at 30% recovery. The difference between the 22% reduction in a module-scale test and the 50% theoretical reduction in SEC for RO is partly explained by the low RO recovery, 30%, which results in a lower concentration brine.

5. High-pressure membrane performance

Recovering energy from high-concentration brines requires much higher hydraulic pressures than seawater PRO. In practice, PRO membranes suffer from deformation and reduced effectiveness as draw concentration and applied pressure increase (Achilli et al 2009, Straub et al. 2015, and Han et al. 2015). Straub and

coworkers investigated the performance of a polysulfone thin film composite (TFC) membrane supplied by Hydration Technology Innovations (Albany, OR) at concentrations ranging from 0.6M to 3M NaCl and pressures from 0 to 48.3 bar. Scanning electron microscope (SEM images of the membrane at low (13 bar) and high (55 bar) pressures showed significant deformation increasing with pressure (Straub et al. 2015).

Operational tests of the polysulfone membrane sample showed that the membrane structural parameter (S) increased, water flux parameter (A) decreased, and salt flux parameter (B) increased with increasing applied pressure to the draw solution (Straub et al. 2015). Additionally, the feed channel compressed at higher pressures, exacerbating the tradeoff between feed channel pressure losses and concentration which is controlled by the feed channel pressure and flow rate (Straub et al. 2015). The reverse salt flux was found to increase significantly with both increasing draw concentration and hydraulic pressure, suggesting that in PRO configuration, B cannot be assumed constant (Straub et al. 2015). Li and coworkers (2015) also calculated A, B, and S, finding that each parameter varies with applied pressure. In their study, a polyetherimide (PEI) PRO flat sheet membrane was synthesized and tested for performance under conditions designed to simulate concentrated RO brine (Li et al. 2015). The PEI (2 synthesis treatment) exhibited a power density of 12.8 W/m^2 at 17.2 bar with 1M saline and deionized feed water; the measured salt permeability was 0.87 LMH, lower than other reported results (Li et al. 2015). Membranes for RO-PRO application should be able to withstand draw concentrations of approximately 1M NaCl and applied pressures above 20 bar.

6. Fouling

In addition to physical membrane deformation, fouling, pretreatment, and cleaning cycles are a major concern in RO-PRO applications (Saito et al. 2012). Fouling is primarily a concern for building and operating a pilot system and for evaluating the viability of scaling up to commercial operation. Fouling reduces energy recovery by diminishing the flux through the membranes. In the first pilot-scale physical test of RO-PRO with RO brine and treated wastewater feed, it was found that conventional wastewater treatment plus UF pretreatment was insufficient to prevent membrane fouling in PRO mode (Saito et al. 2012). Low-pressure RO pretreatment of the treated wastewater significantly reduced fouling, but it required a large energy input (Saito et al. 2012). Recent tests of fouling effects and control demonstrate that both inorganic and organic species deposited within the porous structure could not be easily removed by hydrodynamic methods of backwashing (D. Kim et al. 2015). A synthetic wastewater sample was prepared with inorganic foulants (to represent scaling factors) and organic foulants (D. Kim et al. 2015). Sodium alginate, bovine serum albumin (BSA) and Suwannee River natural organic matter (SRNOM) were chosen as model organic foulants to respectively represent the polysaccharides, proteins, and NOM found in typical municipal wastewater (D. Kim et al. 2015). In their tests with a CTA flat sheet membrane, inorganic scaling was found to be the primary cause of PRO fouling, and an anti-scaling agent significantly increased flux through the membrane (D. Kim et al. 2015).

7. Pilot efforts

Wan and Chung (2015) fabricated polyethersulfone (PES) hollow fiber membranes for a bench-scale analysis of the membrane performance in PRO configuration (Wan and Chung 2015). The hollow fiber membranes were tested with 2 sets of inputs: deionized feed and 1M NaCl draw solution as well as RO brine from the TuaSpring desalination plant and tertiary-treated wastewater (NEWater) (Wan and Chung, 2015). Changing the draw solution from 1M NaCl to RO brine made negligible changes to water flux rates while replacing the deionized feed with NEWater resulted in a 75-80% reduction in water flux (Wan and Chung 2015). Ultrafiltration (UF) and nanofiltration (Chen et al. 2016) were both tested for reduction of foulant constituents as well as improvement of flux rates. UF was found to be somewhat effective at removing organics, while NF effectively removed organics and some scaling agents (Wan and Chung, 2015). As applied pressure increased with the NF-treated NEWater feed, flux also increased through the membrane: the best case scenario occurred at 20 bar, resulting in a power density of 8.9 W/m^2 and a flux rate 59% lower than that attained with deionized feed (Wan and Chung, 2015). They concluded that both organic fouling and scaling diminish water flux with real wastewater: membrane-appropriate anti-scaling agents are necessary to improve performance further, and NF effectively removes organics, but costs 5 bar operating pressure (Wan and Chung, 2015).

III. OBJECTIVES

The primary focus of this investigation is a pilot-scale process optimization study performed at Samoa, CA using a commercial-scale pilot designed and built for this purpose by Cal Poly Humboldt and funded by CA Department of Water Resources with assistance from Oasys, Inc, and the Humboldt Bay Harbor District. Constructing and operating a pilot-scale test facility is crucial to exploring the opportunities and limitations of current PRO technology at the process level, rather than laboratory bench-scale. Previously, pilot studies have focused on exploring *membrane capabilities* for reclaiming energy in the PRO subsystem—the primary metric of evaluation has been power density (W/m^2). This study focused on exploring *operating strategies* to minimize energy consumption for purifying freshwater from seawater in a pilot-scale RO-PRO system—the primary metric for evaluation was kWh/m^3 of freshwater produced from seawater. The entire RO-PRO process, including RO pressurization, circulation, and energy recovery, as well as PRO circulation and energy recovery, was included in this specific energy consumption analysis. Operating parameters for minimum energy consumption in a system of full-scale modules may differ from parameters designed to achieve peak power density which represent the best conditions for a discrete section of membrane. Prior evaluation of PRO has proposed that PRO must be able to achieve 5 W/m^2 power density in order to achieve commercial viability (Skilhagen, 2010). Important questions were:

1. Can this pilot scale system achieve a PRO power density of 5W/m^2?
2. What will the power density be when the pilot is operated at system-wide optimal conditions?
3. Using bench-scale membrane performance values for PRO and commercial scale pump and device efficiencies, PRO could significantly reduce energy costs for RO desalination, thereby reducing environmental impacts, GHG emissions, and operating costs?

This pilot-scale investigation explored the current limits for PRO energy recovery in a seawater RO facility using 4040 commercial membrane modules. The number of PRO modules, RO recovery rate, PRO flow path, PRO flow rates and operating pressures for feed and draw solutions were all tested at the pilot facility to inform optimal operating conditions.

This study aims to minimize energy consumption from producing freshwater using an RO-PRO combined system. Due to lack of availability of miniaturized pressure exchanging (PX) devices, the pilot system was not able to directly measure energy consumption in an RO-PRO-PX system. Instead, flow rates and pressures were measured in an RO-PRO system, and standard efficiencies for pumps and PX devices were applied where each device is necessary in the RO-PRO-PX design schematic (Figure 2). Minimizing energy consumption in an RO-PRO-PX system is a multi-variable effort. To simplify, pumping efficiencies and PX device efficiencies are held constant. Flow rates, flow paths, pressures, RO recovery rates are all varied. At its core, this energy minimization problem reduces to the following goals:

1. maximize freshwater recovery in the RO system
2. maximize freshwater flux (permeate) in the PRO system
3. maximize operating pressure in the PRO draw stream
4. minimize pressure losses due in both RO and PRO systems

The design goals for the pilot are to create a linked RO-PRO system that is capable of testing a wide enough range of recovery rates, flow rates, and pressures to find global minimum energy consumption and best operating points (BOPs). BOPs may not coincide with the global minimum because they are constrained by commercial equipment and commercially-feasible RO recovery rates of freshwater from seawater.

IV. METHODS

Section 1 of Methods discusses design of an RO-PRO-PX system, starting with theoretical design, modeling results, and practical design of the pilot system built at Samoa, CA. Section 2 details the optimization strategy and methodology for establishing BOPs.

1. RO-PRO design

A. Theoretical design

The linked RO-PRO system design was conceived by Achilli and coworkers (Achilli, 2009) and physical tests in a full-size system were first conducted in Japan (Saito et al., 2012). In an RO-PRO system, the work produced by PRO is transferred directly from the pressurized PRO draw solution discharge to the incoming RO seawater using an energy recovery device (ERD) (Saito et al., 2012). In this project, a seawater RO system, with four Dow Filmtech SW30-4040 modules and an industry-standard ERD, was designed to discharge brine directly to an array of 4040 PRO modules. Energy is gained when the PRO discharge pre-pressurizes part of the RO feed water through an ERD, see PX1 in Figure 2. Seawater enters the system on the left of Figure 2, and part of the flow is pressurized to the RO operating pressure, while the remainder passes through a series of ERDs (PX1, PX2) before being boosted to the same RO operating pressure.

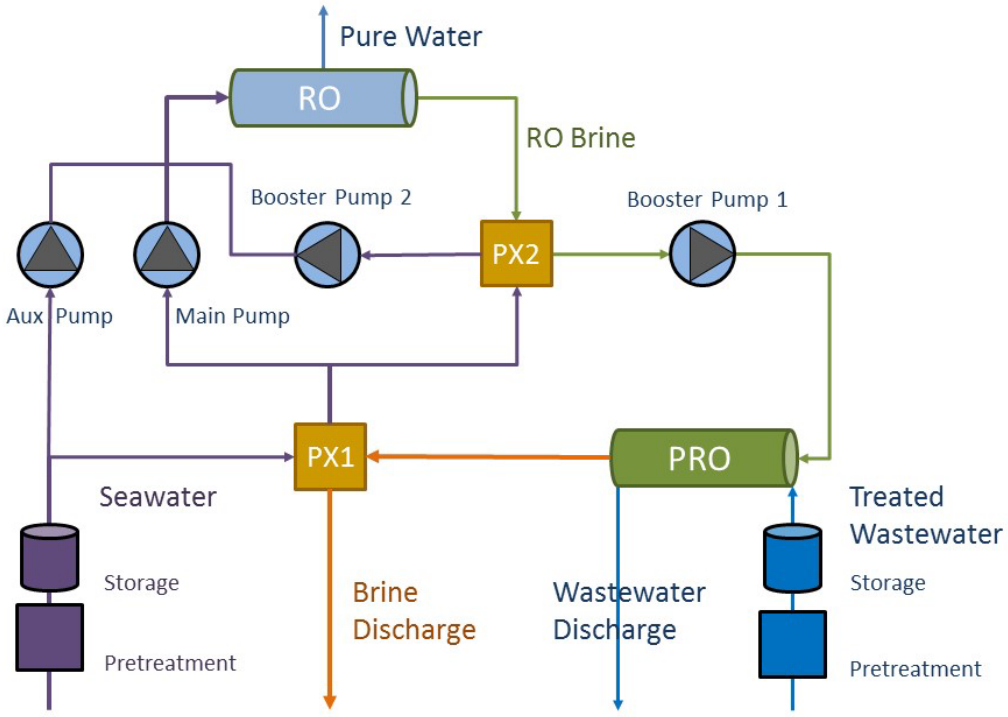

Figure 2: Seawater enters the system on the left, and part of the flow is pressurized to the RO operating pressure, while the remainder passes through a series of energy recovery devices (PX1, PX2) before being boosted to the same RO operating pressure. The RO brine exits PX2 and the pressure is boosted to the PRO operating pressure (top right). PRO feed water, shown here as treated wastewater, fluxes through the PRO membranes and increases the pressurized flow. The pressure from all of the PRO discharge is transferred to the incoming seawater at PX1, before being discharged back to the sea The RO brine exits PX2 and the pressure is boosted to the PRO operating pressure (top right).

PRO feed water fluxes through the PRO membranes and increases the pressurized brine flow. The pressure from the now-diluted PRO brine is transferred to the incoming seawater at PX1, before being discharged back to the sea. The design goal is to minimize the SEC_{net} consumption of the RO-PRO system by diluting the brine and recovering energy from the exiting pressurized fluid.

B. Modeling of thermodynamics for RO and PRO

The physical RO system design was based on modeling using the DOW Chemical Company software, ROSA (Reverse Osmosis System Analysis). This initial modeling provided starting points for energy consumption, operating pressures, and estimated brine quality for the RO discharge to the subsystem. These modeled parameters were also used to provide inputs for PRO modeling and initial operating points for the effort to minimize energy costs for operating the physical system. Both 40% and 50% RO recovery were modeled to determine operating parameters for the RO-PRO system with a feed water concentration of 35.0 g/L NaCl. The ROSA analysis also provided the SEC of the RO system. In a standalone RO system without energy recovery, the SEC can be calculated as in Equation 5:

Equation 5. $$SEC = \frac{\Delta P_{RO} * Q_f}{\eta_{pump} * Q_p} = \frac{\Delta P_{RO}}{\eta_{pump} * Y}$$

Where:

ΔP_{RO} = $P_6 - P_1$, the operating pressure of the RO system
Y = the RO yield Q_p / Q_f
η_{pump} = pressure pump efficiency

The PRO system (Figure 5) was designed based on outputs from a Fortran 90 program previously developed (O'Toole et al., 2016) using a non-ideal transport model developed by (Achilli et al. 2009). The model estimated specific energy, discharge pressures, permeate targets, and initial flow rates.

For an RO-PRO system (Figure 2), two pressure exchangers and a booster pump are added to transfer energy to the RO feed stream, Q_T. The efficiency of the pressure exchangers is applied to the pressure difference between the two feed streams for each PX device. The energy recovered by the PRO subsystem (SE_{PRO}) and pressure exchangers (SE_{boost} and SE_{pump}) is represented in Equation 6, Equation 7 and Equation 8, respectively. Equation 9 represents an auxiliary pump (pump 3 in Figure 2) which is added to maintain the RO feed rate when the PRO permeate is less than the RO permeate.

Equation 6. $$SEC_{PRO} = \frac{\Delta P_{PRO(out)} * (Q_{p(PRO)})}{Q_p} - \frac{P_{PRO(feed)} * Q_{Win}}{Q_p} + [\frac{P_{PRO(out)} * Q_t * \eta_t}{Q_p}]$$

Equation 7. $$SEC_{boost\ PX} = \frac{(P_b - P_{PRO(in)} * \eta_{PX2}) * Q_b * \eta_{PX1} * \eta_{boost}}{Q_p}$$

Equation 8. $$SEC_{pump\ PX} = \frac{(P_{RO(in)} - P_{PRO,out} * \eta_{PX2}) * (Q_f - Q_b) * \eta_{pump}}{Q_p}$$

Equation 9. $$SEC_{RO(aux)} = \frac{\Delta P_{RO} * Q_y}{Q_p * \eta_{pump}}$$

Where:

ΔP_{PRO}	=	$P_2 - P_1$, the residual operating pressure of the PRO system
$Q_{p(PRO)}$	=	the PRO permeate flow rate ($Q_{Win} - Q_{Wo}$)
$P_{PRO(feed)}$	=	feed pressure of Q_{Win}, P_7
$P_{PRO(in)}$	=	inlet operating pressure for the PRO system, P_3
η_{boost}	=	booster pump efficiency
η_{PX}	=	pressure exchanger efficiency
Q_t	=	$Q_{p(PRO)} - Q_p$, when dilution is greater than recovery
Q_y	=	$Q_p - Q_{p(PRO)}$, when recovery is greater than dilution

The final term in Equation 6 has a value of zero unless the PRO permeate is greater than the RO recovery. It is important to note that highly-efficient pressure exchangers require equal flow of water for high- and low-pressure inputs—creating a set of system equilibrium points when RO recovery = PRO permeate.

The SEC of the RO-PRO-PX system (Equation 10) is modeled as the combination of Equations 3 – 7, where Q_f includes Q_y (Figure 2) when recovery is greater than dilution.

Equation 10. $$SEC_{RO-PRO-PX} = \frac{\Delta P_{RO} * Q_f}{\eta_{pump} * Q_p} + SEC_{RO(aux)} - SE_{PRO} - SE_{brine\ PX} - SE_{pump\ PX}$$

Pretreatment energy costs and the effects of fouling are not included in this analysis. PX efficiency is assumed to be 96%, the pump efficiencies are assumed to be 80%. The target RO yield and the PRO permeate are balanced at Y = 40% and dilution = 40%, respectively. When Y equals dilution, Q_y and Q_t (Figure 2) are equal to zero.

The combination of outputs from ROSA and the Fortran 90 program provide initial/expected operating pressures, flow rates for the RO and PRO system, and the number of PRO modules necessary to achieve 40% dilution. The estimated PRO permeate rate from modules in parallel and in series is used to determine the number of modules necessary to achieve 40% dilution. Due to space considerations and availability, the total number of PRO membrane elements was limited to five. According to model results, six modules were sufficient to achieve 40% dilution at pressures below 100 psi. However, at pressures closer to one half of the osmotic pressure, dilution was lower than 40%. Low dilution (permeate) rates and TMP limitations in the commercial forward

osmosis membrane prevent direct testing of the theoretical best operating point—which lies somewhere in the set of operating points at which PRO dilution equals RO recovery, and PRO TMP is ½ of the osmotic pressure.

C. Computational modeling results

Combined results from ROSA (seawater RO) and the PRO model display reduced specific energy ($SEC_{RO\text{-}PRO\text{-}PX}$, Equation 10) above 20% RO recovery of freshwater from seawater (Figure 3). These results suggest that the proposed RO-PRO pilot should be

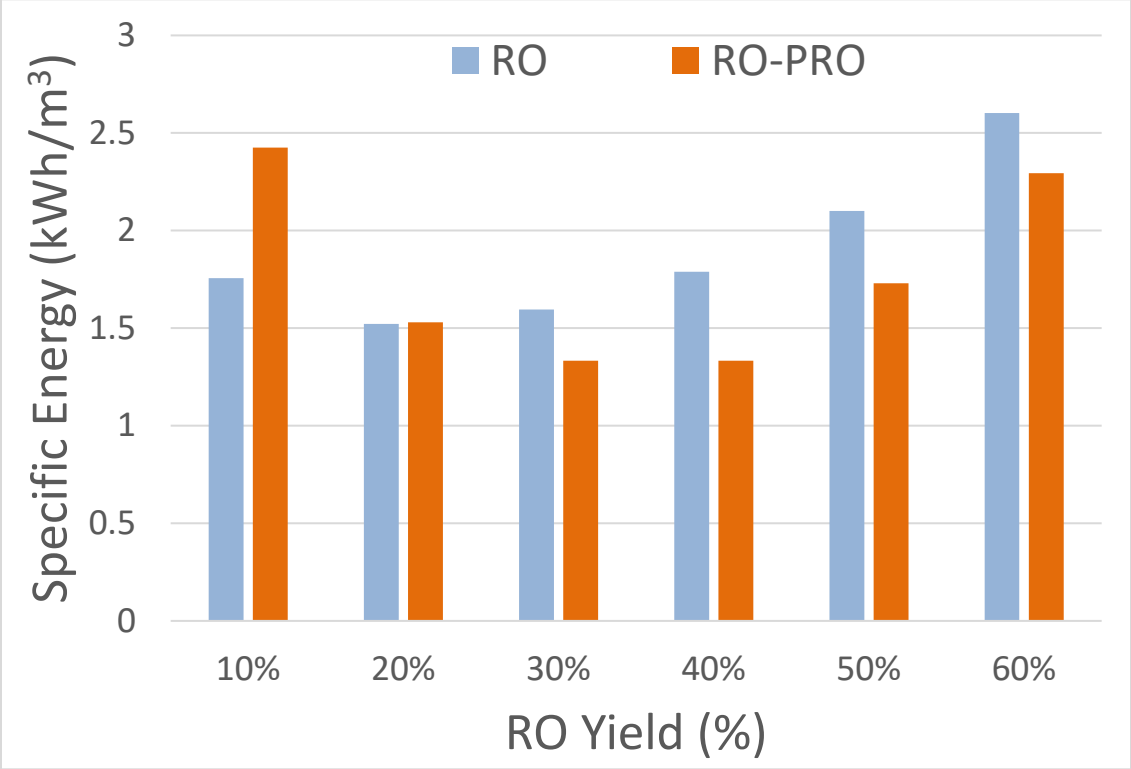

Figure 3: Specific energy of freshwater produced from seawater via reverse osmosis, with energy recovery delivered by PRO modules operating at dilution equivalent to RO yield. For example, at 40% RO yield, PRO dilution would also be 40%--salinity of PRO outputs would be similar to the salinity of the seawater feed stream.

capable of up to 50% RO yield, and ideally up to 50% PRO dilution. Due to the current commercial quality of membranes, 50% RO yield should be achievable on a pilot scale, whereas 50% PRO dilution may not be currently feasible with commercial equipment. An additional goal then becomes maximizing the PRO dilution through operating parameters.

2. Site characteristics

A. Location

The Samoa Pulp Mill is owned by the Humboldt Bay Harbor District and spaces are leased out to various businesses including aquaculture and culinary salt production. The site is located across Humboldt Bay from Eureka, CA, near the inlet to the Bay (Figure 4). Bay water quality is heavily influenced by ocean water quality and interchanges frequently. In general, high tide water quality is negligibly different from the ocean, while low-tide water quality is more heavily influenced by silt from mud flats and evaporation in the shallow North Bay. The Humboldt Bay Harbor District leased a small space in the old Pulp Mill for the RO-PRO system and provided electrical utilities, freshwater, seawater pumping and conveyance, and maintenance staff to help set up tanks and utilities for the pilot.

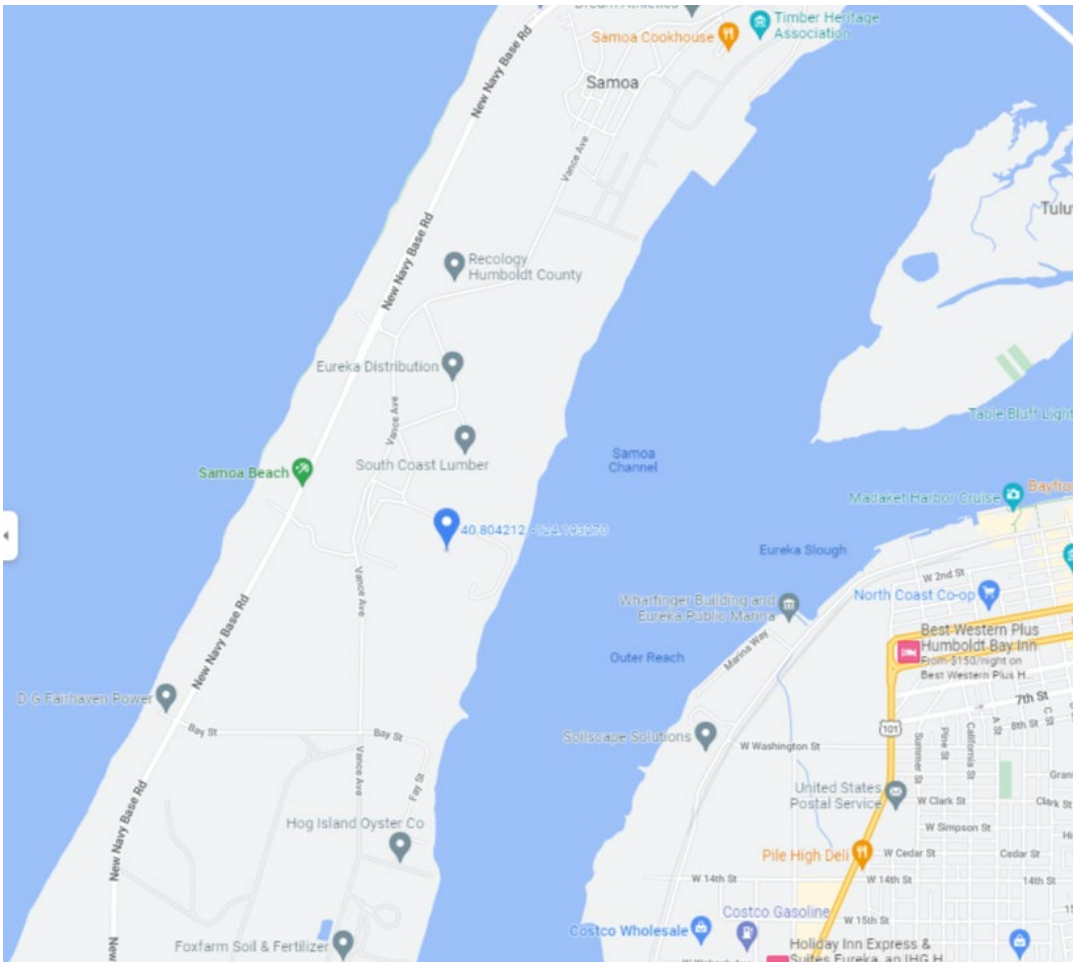

Figure 4: RO-PRO pilot location (blue pin marker at center) at the Samoa Pulp Mill near Eureka, CA. Map courtesy of from Googlemaps.com

B. Humboldt Bay water quality

In general, Bay water quality was assumed to be similar coastal ocean water quality, as monitored and recorded through local NOAA buoy stations. It was also assumed that there may be higher sediment and algae in the Bay water than typically recorded at the nearby buoy locations. Pre-treatment is always necessary for surface water prior to provide high-quality feed water for the RO system to prevent fouling and short-term drops in performance. Water quality tests were performed for biological

oxygen demand (BOD_5), total dissolved solids (TDS), total suspended solids (TSS), and conductivity. Averaged results from water quality tests (Table 1) were used to inform the design of seawater pre-treatment.

Table 1: Water quality results for grab samples taken from the pier at Samoa Pulp Mill, adjacent to seawater extraction point. Samples were collected on three different days from March through May 2017. Mention Standard Methods and YSI conductivity probe

Test	**Value**	**Units**
BOD	~2.2	mg O_2/L
TDS	35.2	g/L
TSS	35.0	mg/L
Conductivity	48	mS/cm
TDS/conductivity	0.733	(g/L)/(mS/cm)

Overall, water quality measured to be favorable for RO, and TDS is very close to nearby NOAA monitoring stations in the ocean.

C. Pre-treatment design

Timing and screening

The pilot was run in batches from a tank of treated seawater, and water was withdrawn from the bay in batches as well for pre-treatment. The intake pump was placed far out in the Bay on a pier, and water was pumped on near high tide on the incoming and slack tides in order to take in the best quality water. The pump intake was wrapped with screen mesh to prevent debris and bits of seaweed from entering the intake line.

Primary filtration

Seawater requires filtration and treatment prior to RO membranes, while freshwater, withdrawn from the tap, is expected to be clean, but can still pick up pipe debris, scale flakes, and other solids in aging water pipes. Water from the seawater intake

was conveyed in a pipe to the pilot system, where water passed through a series of three cloth cartridge filters: 20 µm – 5 µm – 1 µm. After each seawater withdrawal of 2,000 to 3,000 gallons, the cartridge filters were removed and washed off before storing to prevent biological growth and permanent fouling of the cloth filter media. Freshwater influent was filtered through a 0.5 µm carbon block filter to remove pipe debris, chlorine residual, and any fine sediment that might clog the PRO membranes.

Coagulation

Samples of seawater were taken from adjacent the intake location on the pier, and two rounds of coagulation jar tests were performed with ferric chloride and alum in a range of doses. During the second round, the incremental dose was smaller in each test and focused on the best-performing doses from round 1. Alum and ferric chloride had similar results, and Alum was chosen as coagulant due to lower toxicity and safer materials handling. A ratio-driven mechanical injector was purchased to deliver coagulant to seawater after primary filtration, and before entering a 300-gallon mixing tank. The goal with a short residence time mixing tank was to create a micro-floc that would improve removal in the subsequent ultrafiltration system.

Ultrafiltration

A hollow-fiber HYDRAcap 40-LD system by Nitto Hydranautics was borrowed from University of Nevada Reno for the pilot duration. The system arrived disassembled, with missing parts and a non-functioning control board. After some effort, a new hollow fiber module, and consulting with a control systems professional, the system was operational and functioned smoothly for the pilot testing. Water quality exiting the

system exceeded minimum parameters for RO membrane operation, and the RO system performed consistently without loss of performance during the pilot tests. Seawater was stored in a 4,000 gallon tank after ultrafiltration. Ultrafiltration removes most bacteria and algae, so the stored water quality was expected to have minimal growth in the tank and maintain high quality. In practice, no visible growth was detected in seawater coming from the tank to the RO system.

Antiscalant

Antiscalant was added to the seawater between the storage tank and the seawater RO membranes in the pilot system. FlowCon 135 antiscalant was added at a rate of 0.01% V/V to the seawater feed stream to the pilot system. This was achieved by diluting the FlowCon 135 by 1/10 in a dosing bucket, and then providing the minimum dose of 0.1% V/V through a MixRite proportional injector.

3. As-built design and construction

In 2016, construction began on an RO-PRO facility with pumps, control systems, electrical, and membrane modules housed in a small, enclosed trailer. The design was based on earlier efforts by Achilli and colleagues at University of Nevada Reno (Achilli, et al. 2014). Additional elements were added to the design to employ pressure exchangers, treat seawater for RO, and test commercial modules in a variety of flow-path configurations. In early 2017, the trailer system was moved to Humboldt Bay Harbor District's old pulp mill site for deployment and operation. Figure 5 depicts the full RO-PRO system, including intake sources and pretreatment as built at the Samoa Pulp Mill in

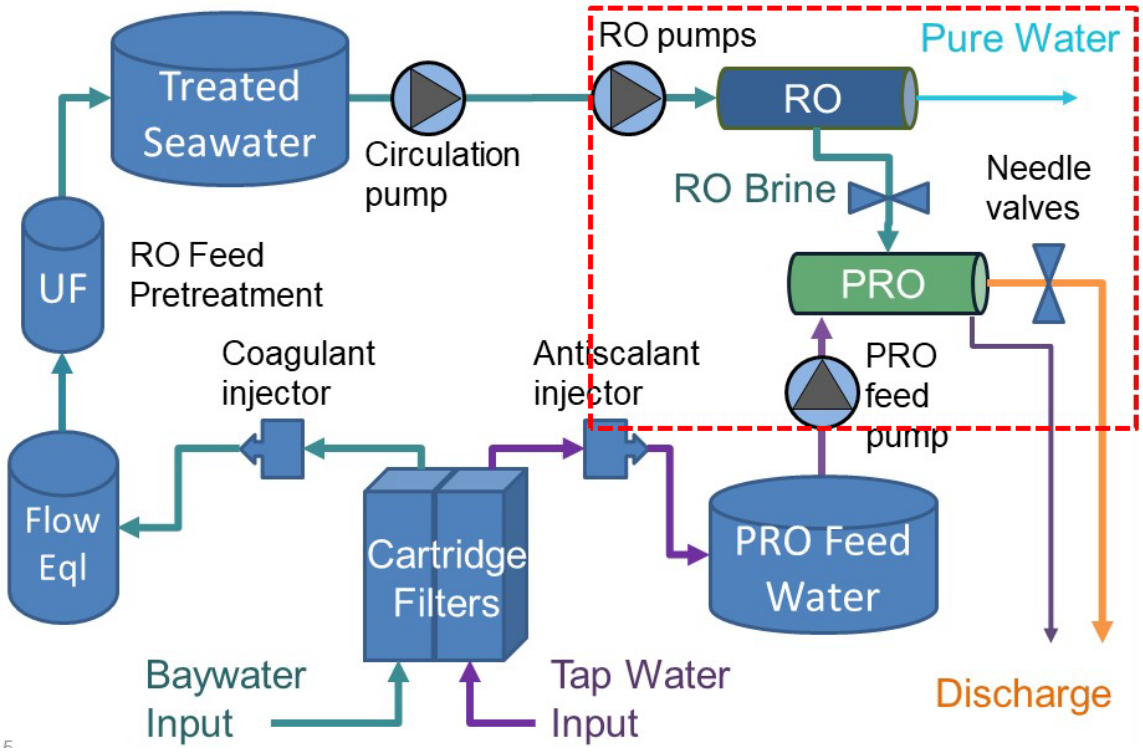

Figure 5: As-built diagram of RO-PRO facility at Samoa Pulp Mill facility. The section outlined in red is inside the trailer, while the pretreatment and storage for freshwater and seawater are both outside the trailer.

Samoa, CA. The area outlined in red is the active RO-PRO membrane system inside the trailer and shown in greater detail in Figure 6. Figure 6 includes two pressure exchangers (PX devices) that were plumbed but never installed due to lack of availability. The system was operated without PX devices—also removing the need for both RO and PRO booster pumps and the seawater auxiliary pump shown in Figure 6. The simplified system without PX devices is shown in Figure 7. Pictures of the system as it was built and set up at the Samoa Pulp Mill are in Appendix A in Figures 18-22.

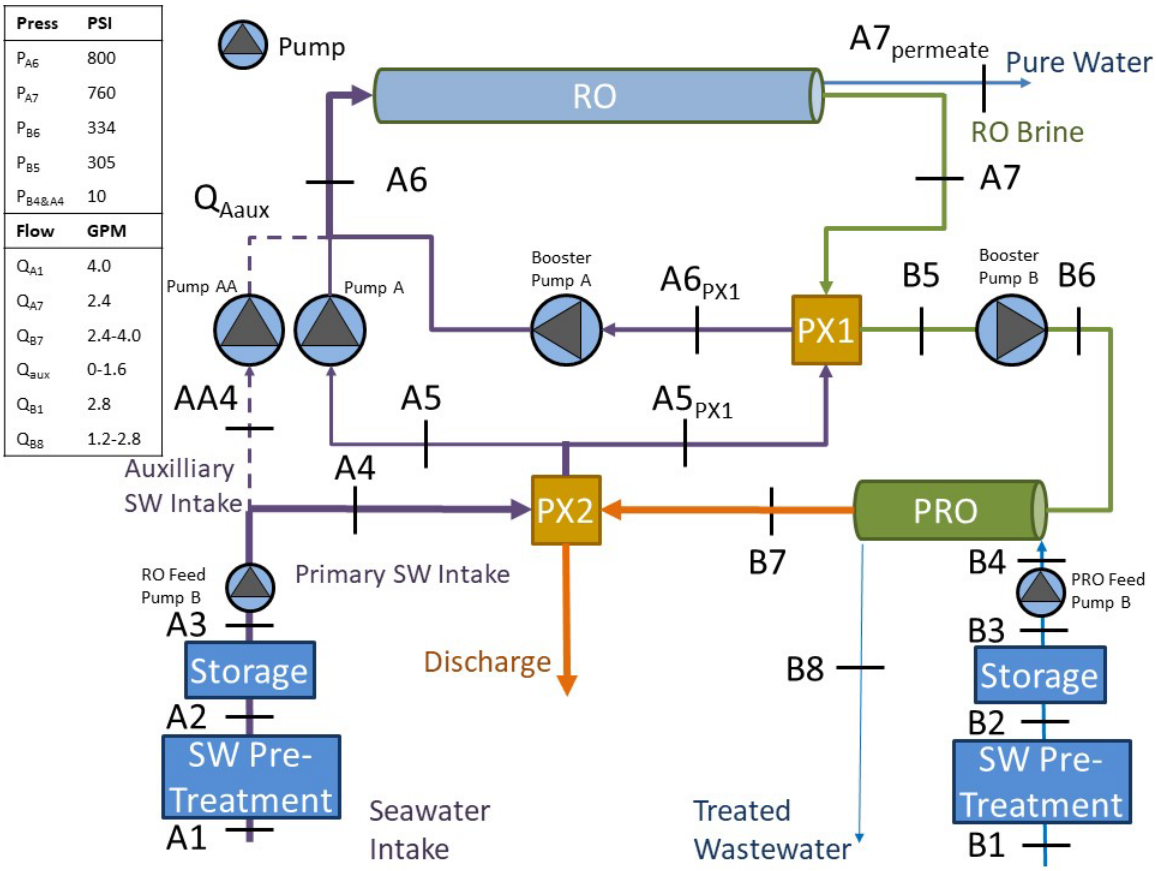

Figure 6: RO-PRO-PX system as built at Samoa, CA. The system was never operated in this configuration due to unavailable PX devices and was simplified to Figure 7 for operation. Inset values are from model outputs operating at 40% RO recovery.

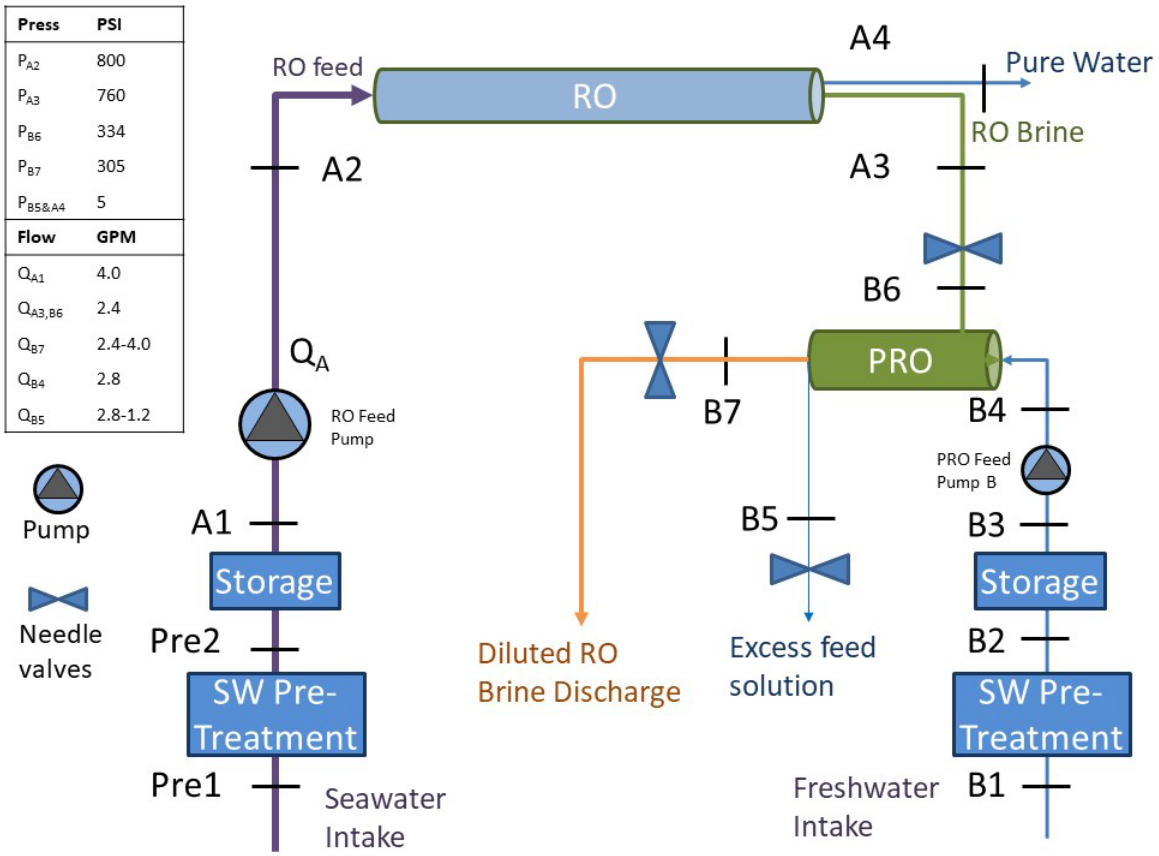

Figure 7: The full as-built diagram in Figure 6 was simplified to this configuration for testing and operation due to lack of available PX devices. Inset values are modeled expectations for 40% RO recovery and operating at ½ π. The Oasys forward osmosis membrane used in the PRO system were unable to withstand greater than ~220 psi, so this configuration was only tested with pressures up to 220 psi.

The seawater RO system consisted of a high-pressure pump and four 4040 SW30 Dow RO membranes arranged in series. This system was capable of consistently producing 50% recovery from Humboldt Bay seawater. The design flow rate was chosen at approximately the minimum of 5.0 gpm for these modules, as provided by modeling analysis with ROSA. Below 5.0 gpm would yield insufficient feed water to flush the final module—risking mineralization on the membranes at the tail end of the RO system.

The PRO system consisted of five 4040 Oasys forward osmosis (Company) membranes plumbed in PRO mode, with the draw side containing residual pressure from the RO system as controlled by the needle valve at B6 in Figure 7. The five FO membranes were plumbed with valves and a pipe network to allow for several different flow configurations. Draw could be in series or parallel, and feed could be in series or parallel as well.

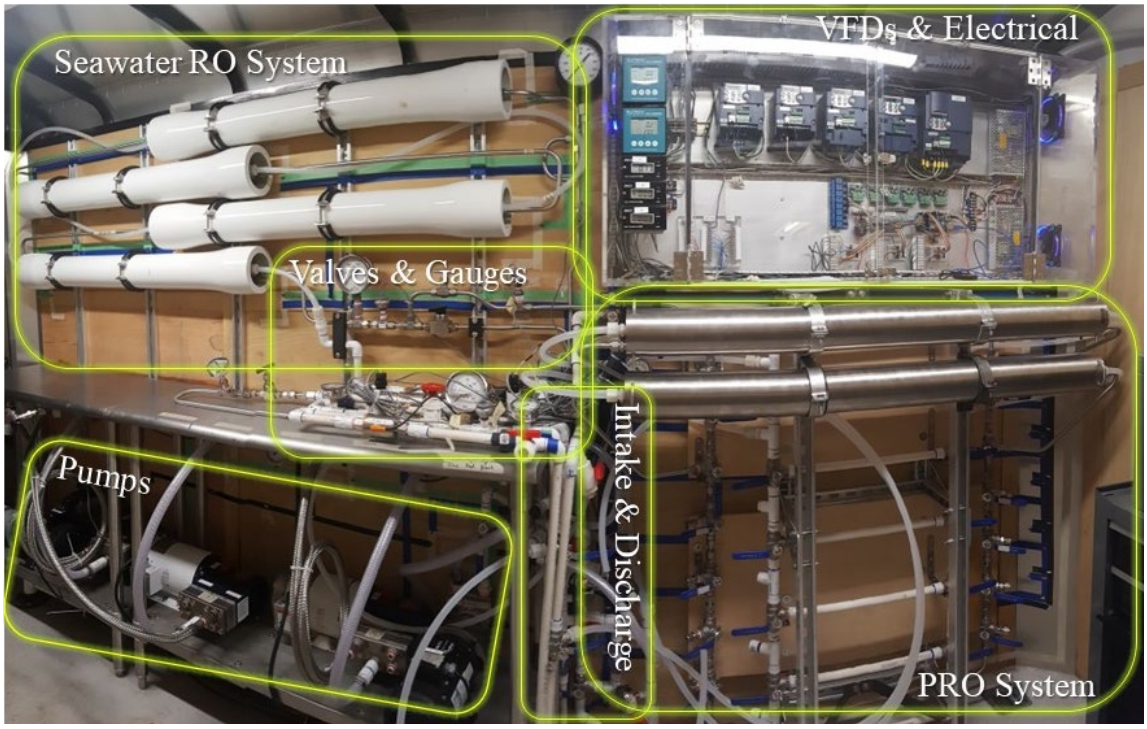

Figure 8: RO-PRO membrane system as operated at Samoa Pulp Mill facility. Upper left shows four seawater RO modules; upper right shows an electrical control panel with VFDs and electronic sensors; in the center is a cluster of pressure gauges, sensors, and manual control valves; lower right are connections for up to six PRO modules; bottom center are vertical discharge and intake pipes, and the pumps are in the lower left on a steel-reinforced shelf. An Arduino is situated in the electrical control panel that is capable of controlling the pumps via VFDs based on sensor inputs. This picture shows only two membrane modules (lower right) installed for preliminary testing. For the main experiments, five modules were installed.

Building and deploying this system at the Samoa Pulp Mill required careful coordination with the Humboldt Bay Harbor District, utilities, storage tank installation, plumbing, and careful investigation of freshwater and seawater supplies (Table 1).

4. Testing and optimization methodology

To determine whether there is a set of operating conditions for the pilot that can achieve 25% energy savings for RO at the commercial scale various operating points were evaluated, Pilot system testing is designed to catalog a set of operating points as close to the theoretical optimal points where RO permeate = PRO permeate, ΔP_{PRO} = ½ osmotic pressure, and SEC of RO-PRO-PX is lowest within a feasible commercial range of operation, i.e., between 40-50% RO recovery. By capturing achievable operating conditions closest to the theoretical maximum PRO power and minimum SEC_{RO}, we hope to also display the optimal (minimum) energy ($SEC_{RO\text{-}PRO\text{-}PX}$) required for producing freshwater in the RO-PRO system.

Thermodynamic efficiency of the RO-PRO system was measured via the following variables:

4. RO flow rate
5. RO yield rate
6. PRO transmembrane pressure (TMP)
7. PRO membrane area
8. PRO feed solution flow rate
9. PRO draw solution flow rate
10. PRO operating configuration
11. PRO dilution, or permeate rate

A. Optimization Strategy

The strategy follows the objectives: maximize RO yield, maximize PRO permeate, maximize PRO draw pressure (TMP), and minimize energy cost of pumping.

Variables

1) RO yield rate is limited by the pilot-scale RO system. While recovery of 50% is possible, operating at 40% recovery yields improved system stability for the pilot system of four 4040 RO modules arranged in series. As RO yield increases from 10% to 50%, the discharge brine (PRO draw solution) decreases in flow rate and increases in salinity. Lower draw flow rates reduce friction energy losses in the pipes and PRO modules, and higher salinity increases the theoretical optimal TMP and improves PRO permeate rates if pressure is held constant.

2) Transmembrane pressure (TMP): increasing PRO operating pressure for the draw solution provides more power (energy recovery) as PRO feed pressure is held constant. The difference between average PRO feed and draw pressures approximates the pressure differential between feed and draw solutions experienced by the PRO membrane—this is the transmembrane pressure (TMP). As draw pressure increases, the draw channel space between the spiral-wound membranes is expected to increase, thereby shrinking the feed channel space. As feed channel space decreases, cross-flow feed velocities and pressure losses due to friction will both increase with constant feed flow rate. Additionally, increases in draw pressure will reduce permeate through the PRO membrane, thereby resulting in additional increases to average feed flow velocities and friction losses in the feed channel.

3) PRO membrane area: as the number of PRO modules increases, PRO yield/permeate also increases. Pressure loss due to friction also increases with each additional module, causing a tradeoff—there should be some ideal number of modules

that will balance energy recovered by the PRO system due to improved yield with energy lost due to increased friction by adding another module. If modules are only added in series, this is a simple two-variable equation. However, the pilot-scale PRO system allows for either or both the PRO draw and feed solutions to be operated in series or parallel. If four modules are

4) PRO feed solution flow rate controls cross-flow velocity in the feed membrane channels. As PRO feed velocity increases, PRO dilution rate, and pressure losses due to friction also increase. Higher dilution rate improves system efficiency, while higher friction losses decrease efficiency. There is assumed to be some optimal feed flow rate for a specific membrane module that will achieve the best tradeoff between dilution and friction losses.

5) PRO draw solution flow rate—as the flow rate increases, so does the membrane cross-flow velocity. Higher draw flow rates cause increased pressure losses due to friction and improve PRO draw dilution—PRO permeate increases as cross-flow velocity increases. At the same time, salt flux through the membrane increases with increased draw solution velocity because the average concentration adjacent the membrane surface is higher, providing a higher transmembrane concentration gradient between feed and draw.

6) Operating configuration of PRO modules: parallel and series flow paths for draw and feed solutions are both tested. Modeling suggests that arranging modules in series or parallel will achieve similar total SEC values, until some point where the modules in series will produce more friction losses than recovered energy (Figure 9).

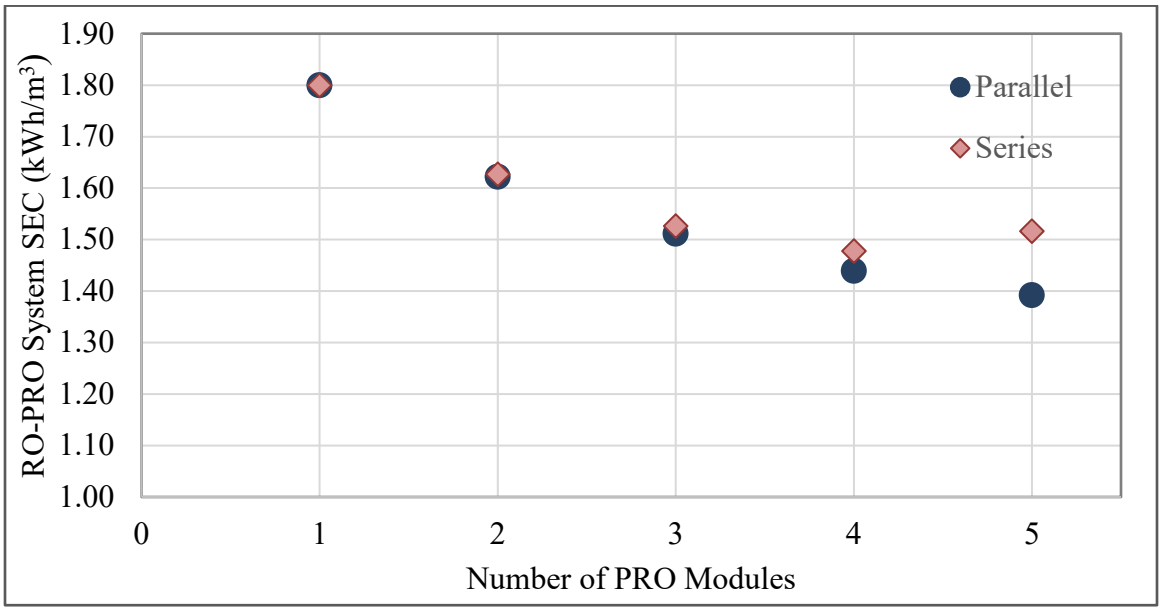

Figure 9: The SEC of the RO-PRO-PX system is plotted versus the number of PRO modules. Increasing the number of PRO modules increases energy recovery for the series configuration until pressure losses overcome the energy recovery due to increased permeate. For the parallel configuration, increasing the number of PRO modules increases the energy recovery with diminishing reductions as additional modules are added.

For pilot experiments, the draw solution was constrained by the best operating point for the RO system, assumed to be 40% RO yield. Altering the flow draw flow rate through the PRO modules, therefore, is only possible by changing the overall system flow rate or changing the draw flow path from series or parallel. In a large PRO system this could be achieved by the flow path; the pumping rate and number of modules in parallel in each successive bank of membrane modules will allow for control over the draw flow rate. In this study, 5 PRO modules were available, so the options are 1, 2, 3, 4, or 5 in series, 5 in parallel, 4 in parallel,2 in parallel followed by two more in parallel, or 3 in parallel followed by 2 in parallel. In initial performance and integrity testing, one of the five membrane modules was found to produce poorer than the rest, so this module was

removed from the system. Testing options were reduced to combinations with 4 modules: 1:1:1:1 or 2:2, for the draw flow path, and 1:1:1:1 or 2:2, for the feed flow path. With a starting flow rate of approximately 3.0 gpm from the RO brine, 4 modules in parallel produced a flow rate below the minimum suggested by the membrane manufacturer, so 4 in parallel was not tested.

7) PRO dilution rate is directly proportional to the flow rate of permeate water through the PRO membranes, also referred to as the PRO dilution rate. Higher flow rate equals higher dilution and higher energy recovery when pressures are held constant. This variable cannot be controlled directly—dilution will increase as a result of increasing draw solution salinity, feed rates and draw rates, and dilution will decrease as TMP increases. Since permeate flux is more commonly used as a benchmark for membrane evaluation, results for flux rates are presented from operating the membranes at various RO recovery rates and TMP values. PRO dilution rate is not a variable that can be manipulated to achieve a best operating point, rather it is an important variable to track to inform design and operating parameters for a facility. How much freshwater will be required to operate the facility effectively? Will booster pumps be required to recirculate the feed water through additional banks of modules to recover as much water as possible before discharge? This series of tests will begin to answer some of these questions for future designers of RO-PRO facilities.

Synthesizing the basic relationships between RO yield, flow rates, salinity, and pressure in the system produces several competing tradeoffs between variables. The goal for minimizing energy consumption (maximizing net PRO energy gained) is to find the

combination of cross-flow velocities and TMP that minimizes feed and draw solution pressure losses while maximizing PRO dilution and draw pressure. This suggests that a low operating pressure for feed solution should be coupled with the highest draw pressure that can be achieved within the linear portion of the relationship between PRO dilution over TMP. Theoretically, the PRO dilution should diminish directly proportional to increasing TMP, or simply, draw solution pressure if feed solution pressure is held constant. In performance tests of Oasys FO membrane modules operated in PRO configuration, there is approximately a linear, direct relationship between PRO dilution and TMP, at lower pressures, up to some threshold. After that threshold, PRO dilution diminishes more rapidly with increased TMP, yielding diminishing energy returns on further increases in draw solution pressure.

Conceptual increments for RO-PRO system tests

The overall strategy for optimizing operation of the RO-PRO pilot was to test the full range of system capabilities. Initial testing moved through the range at low resolution (large difference between consecutive data points) in order to establish tradeoffs provided from different variables. Initial testing strategy for the five control variables are presented in Table 2.

Table 2: Range of variables to be tested for finding minimum SEC_{net} consumption for the linked RO-PRO system

	RO yield	PRO Dilution	PRO Pressure (psi)	PRO Feed Flow rate (gpm)	PRO Draw flow rate (gpm)
Lower Range	0%	0%	0	2.0	4.33
Upper Range	50%	40%	220	4.6	5.33

	RO yield	PRO Dilution	PRO Pressure (psi)	PRO Feed Flow rate (gpm)	PRO Draw flow rate (gpm)
Increment	10%	NA	50	0.1 – 0.5	0.33
Total number of increments	5	NA	5	5	5

Optimization strategy and tests performed with RO-PRO system

With so many variables, it could be difficult to run enough tests to capture all of the combinations of variables to achieve a best operating point. In practice, however, some of the variables were more independent from other variables. In ROSA modeling, RO flow rate had the largest impact on RO-PRO total SEC, so the decision was made early on to keep the RO input constant at 5.0 gpm, based on ROSA modeling. A first round of tests was performed from the conceptual framework in Table 2, resulting in a series of tests whose goals and operating parameters are outlined in Table 3.

Table 3: Approximately 4 rounds of tests were conducted. Each round of tests contained many testing points, and the system was allowed to reach short-term equilibrium for each testing point before sensor values were recorded.

	Testing Objective	Module Configuration	Fixed Variables	Adjusted Variables
Round 1 Tests, RO recovery at 40%				
Test 1: Membrane Area	testing tradeoff between increased membrane area and friction losses	1-5 modules in series 1, 1:1, 1:1:1, 1:1:1:1, 1:1:1:1:1	Feed flow rate, RO flow rate, RO recovery, PRO draw flow rate	Number of modules in series from 1-5, TMP (adjusted by PRO draw pressure)
Test 2: Feed and Draw Flow Rates	testing tradeoff of increased feed permeate versus friction loss from increased fluid velocity	5 in series: 1:1:1:1:1 Draw in 1:1:1:1, Feed in 2:2 Draw in 2:2, Feed in 2:2	RO flow rate, RO recovery, PRO Draw flow rate, TMP	Feed flow rate, module configuration
Test 3: Module configuration,	reduce friction losses through system and maximize potential energy generated by PRO system	Draw and Feed in series: 1:1:1:1:1. Draw 1:1:1:1, Feed 2:2. Draw 2:2, Feed 2:2.	RO flow rate, RO recovery, PRO draw flow rate,	TMP (draw pressure), feed flow rate
Round 2 tests, RO recovery 10% - 50%				
Test 4: Lowest SEC for RO-PRO seawater desalination	Best operating point (BOP), based on RO recovery and operating pressures	Draw 2:2, Feed 2:2	RO flow rate, RO recovery, PRO draw flow rate, Configuration	RO recovery, PRO draw solution salinity, PRO draw flow rate, PRO draw Pressure

Table 7 in Appendix B displays individual set points for each test. Increments of adjusting each variable in the table generally follow the intended increments displayed in Table 2.

B. Data collection

Data was collected for experiments outlined in Appendix B via hand and electronically. Electronic sensor data was monitored and recorded with an Arduino Mega 2560 and output to a micro SD card in *.csv format. Data was also recorded by hand for analog pressure gages, digital flow meters, conductivity readings, and VFD (pump) with power consumption.

C. Data analysis

For both rounds of tests, the basic metric for comparison was net power consumption of the RO-PRO system. Since RO pressure and flow rates were held constant for most of the Round 1 tests, the focus of Round 1 was primarily on optimizing net power production in the PRO half of the system. Round 2 tests were performed using first round results to optimize PRO input variables and then explore the best operating point for the linked RO-PRO system. The basis for comparison between different points (Figure 6) in the system was potential energy, as measured by flow rate times pressure.

Specific energy, in units of kWh/m^3 of RO permeate (see equation Equation 11 below), is used to compare the different states of the system. The potential power at each point in the system was calculated by multiplying flow rate by pressure. The total energy consumption of the RO-PRO system was calculated according to the layout displayed in Figure 6, assuming that PX devices ($\eta = 0.96$), booster pumps ($\eta = 0.85$) and auxiliary pumps ($\eta = 0.85$) are included with their respective efficiencies. The measured flow rates and pressures in the experimental pilot are used to balance the system as displayed in Figure 6. Energy lost in the RO subsystem and potential energy gained in the PRO

subsystem was calculated according to the following equation and normalized to the RO permeate flow rate:

Equation 11. $$SEC = \sum {Q_i * P_i}/{Q_{permeate}}$$

Where: Q_i is the flow rate at point *i* in the system (Figure 6),

P_i is the pressure at point *i* in the system, and

$Q_{permeate}$ is the flow rate of RO permeate

Each testing scenario was evaluated by this aggregate specific energy value for the RO-PRO-PX pilot system ($SEC_{RO\text{-}PRO\text{-}PX}$). This aggregate specific energy is represented by the sum of the products of RO feed pressure times RO feed flow rate, PRO feed pressure times PRO feed flow rate, and subtracting PRO exiting draw pressure times flow rate. Including pump and pressure exchanger efficiencies with this summation yields Equation 10, and the basis for energy comparison between all tested scenarios.

V. RESULTS AND DISCUSSION

The primary goal of this study is to minimize SEC for the RO-PRO-PX ($SEC_{RO-PRO-PX}$) system built at Samoa, CA. Energy losses are measured from overcoming osmotic pressure in RO and from friction in pipes and membrane modules. Salt flux through the membranes results in a loss of potential energy, but it is assumed to be negligible compared to hydraulic pressure losses. The objectives are to maximize RO yield, maximize PRO permeate, maximize PRO draw pressure (TMP), and minimize energy cost of pumping. Increasing pump power causes increased $SEC_{RO-PRO-PX}$, while decreasing $SEC_{RO-PRO-PX}$ results from reducing pump power (friction losses) and increasing energy recovery by the PRO and PX systems. RO-PX performance and the influence of TMP on PRO power are presented first separately for RO and PRO, respectively, and then RO-PRO results are presented for Tests 1-4 described in Table 3. Results are presented in the following order:

(1) Pump power and SEC_{RO-PX} as a function of RO recovery
(2) PRO and Total pump power as a function of TMP: TMP is predicted to be the primary driver of PRO energy recovery
(3) [Test 1] PRO Power and $SEC_{RO-PRO-PX}$ as functions of membrane area and TMP
(4) [Test 2 and Test 3 combined] Three flow path scenarios (module configurations) test PRO flux and power as functions of PRO feed and draw flow rates
(5) [Test 4] Best Operating Point: $SEC_{RO-PRO-PX}$ as a function of RO recovery, TMP, PRO feed flow rates (velocity)
(6) Hypothetical improvements to $SEC_{RO-PRO-PX}$ that are possible with currently available membrane technology
(7) Error analysis for Best Operating Points

1. RO operating pressure: pump power and $SEC_{RO\text{-}PX}$

Pump power and $SEC_{RO\text{-}PX}$ (Figure 10) both increase as recovery rate increases. Pressure exchangers recover potential energy in the exiting RO brine stream—as recovery increases, pressure increases and the flow of brine (recoverable energy) decreases. In Figure 10, below, RO-PX pumping power is approximately linear, while $SEC_{RO\text{-}PX}$ is exponential. If pump efficiency (set at 85%) is increased, the $SEC_{RO\text{-}PX}$ curve flattens somewhat but remains exponential [not shown]. The exponential increase of $SEC_{RO\text{-}PX}$ is likely due to increasing pump power and decreasing brine volume to offset pumping energy. This trend drives optimal RO recoveries lower in an RO-PX system. However, the costs of building and operating an RO facility cause the optimal RO recovery to fall somewhere between 40% and 50% for built facilities. These measured points (Figure 10) are used as a benchmark for evaluating benefits to SEC in the RO-PRO-PX system.

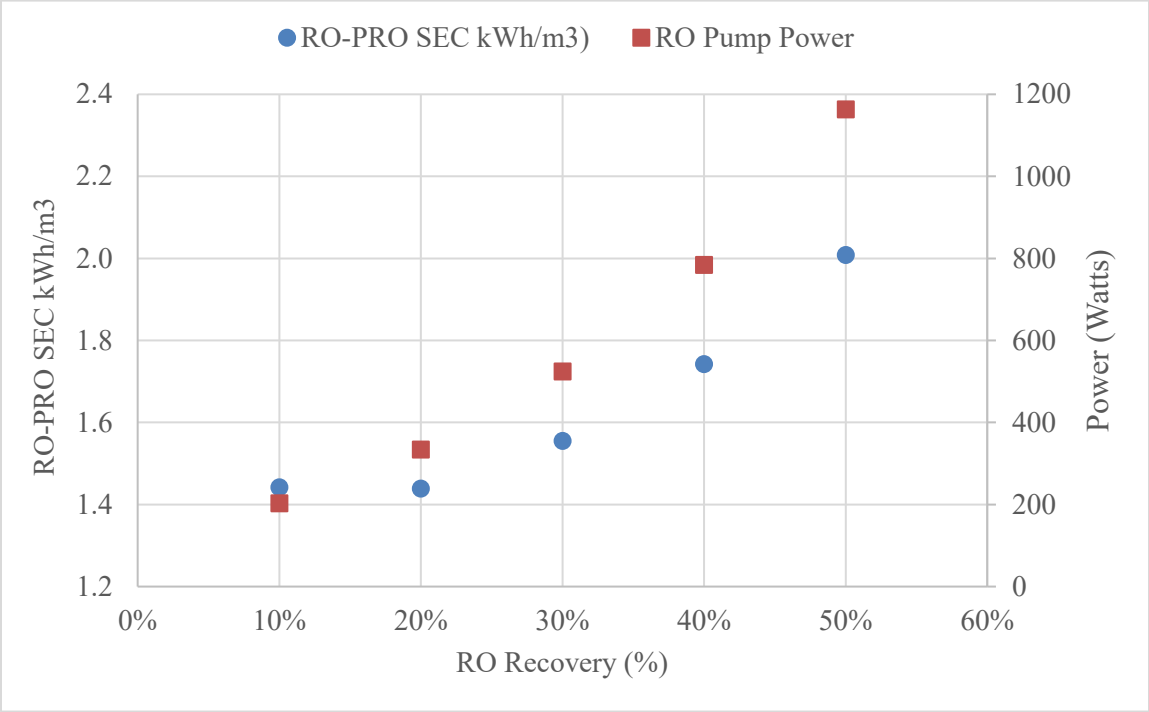

Figure 10: RO-PX specific energy required to produce freshwater permeate from seawater in an RO system increases exponentially with increasing recovery rate when pressure exchangers are included in the system to recover energy from the brine reject stream. Power applied to the pumps (RO primary and booster) increases approximately linearly between 10% and 50% RO recovery.

2. PRO transmembrane pressure (TMP): pump power as a function of TMP in the RO-PRO-PX system

Pumping power increases slightly with increasing TMP in a linear relationship, but the RO recovery rate (salinity of the PRO draw solution) does not affect the relationship between TMP and pump power (Figure 11). This linear increase in pump power will tend to decrease the optimum TMP compared to theoretical peak at ½ of the osmotic pressure.

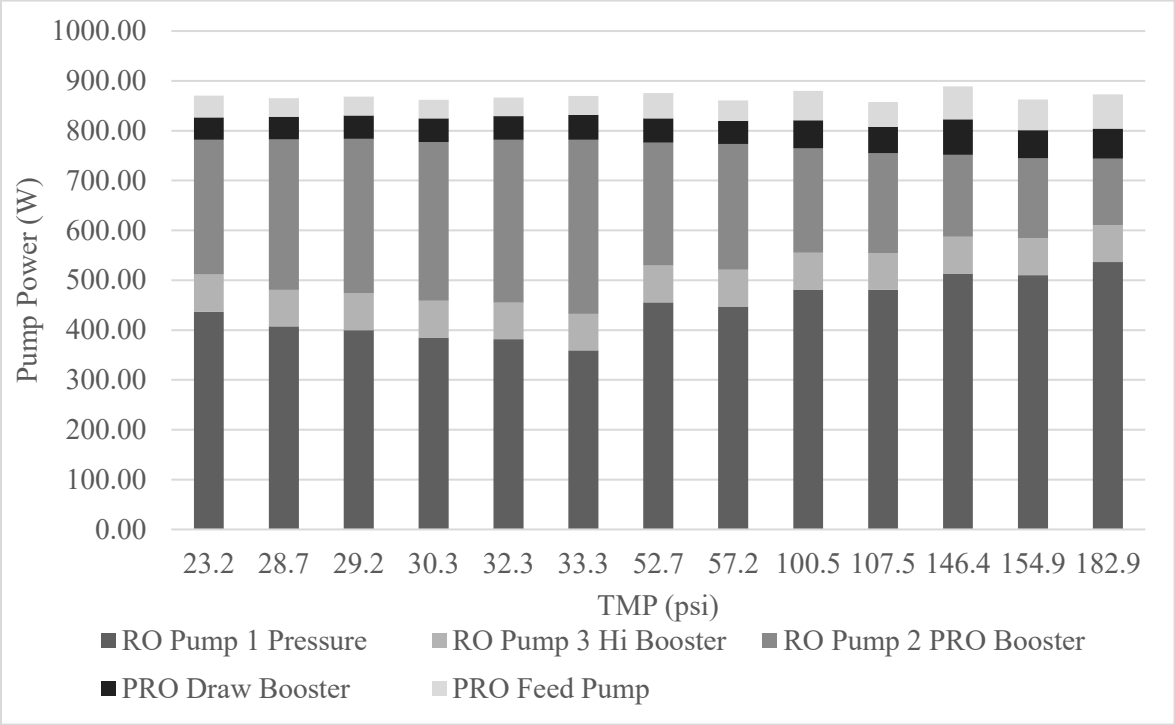

Figure 11: Pump power for each pump in the system is measured as the difference in potential energy (measured pressures and flow rates) between inlet and outlet of each pump multiplied by a pump efficiency of 85%. Calculations assume Pressure exchangers are included in the system with an estimated efficiency of 96%. Total pump power remains approximately constant as transmembrane pressure (TMP) increases. As TMP increases, dilution of the PRO draw stream decreases, causing the initial RO pump to handle more of the total flow to the RO system. The proportion of flow that moves through the PRO system (captured in this figure by RO Pump 2 – PRO Booster) diminishes and the pressure difference between PRO_{OUT} and RO_{IN} also decreases, causing power required by RO Pump 2 to drop.

According to theory, pump power would be expected to diminish as TMP increases, due to potential energy gained by the PRO module(s). This is not evidenced in the pilot tests due to a much steeper decline in permeate rate through the PRO membranes than expected as TMP increases. At 40% RO recovery, higher brine concentrations in the RO reject (PRO draw) result in slight increases in PRO permeate at

higher pressures, but the slight increases do not significantly improve over-all energy recovery.

3. Membrane area: number of PRO modules in series

Greater membrane area can provide more permeate for recovering potential energy from the RO_{OUT} brine stream. In the pilot test this was achieved by adding PRO membrane modules to the system. Each module contained approximately 4 m^2 of forward osmosis membrane. One to five modules were tested in series over a range of transmembrane pressures at 40% RO recovery, see Figure 12. In general PRO power increases due to increased permeate as membrane area increases, see graph in upper right (Figure 12). However, the flux (permeate per membrane area) decreases as membrane area increases, as can be seen in the lower right graph—this means that each additional module offers less additional permeate. The left-side graph in Figure 12 displays the RO-PRO total system's specific energy consumption, normalized to RO permeate (SEC), as a function of both PRO TMP and membrane area. RO-PRO SEC increases as PRO TMP and membrane area increase. The increases in RO-PRO SEC are primarily due to increasing friction losses as membrane area and TMP increase. As TMP increases, the PRO feed channel in the modules was compressed, causing increased pressure loss on the feed side.

In this pilot test, adding modules in series only increased the total energy cost of producing freshwater, due to diminishing returns of additional modules and increased friction losses. The increases in RO-PRO SEC are primarily due to increasing friction

losses as membrane area and TMP increase. As TMP increases, the PRO feed channel in the modules was compressed, causing increased pressure loss on the feed. Figure 12 displays the tradeoffs for PRO and RO-PRO that result from increasing membrane area by adding modules in series. Flux and power captured by PRO both increase, but friction losses across the additional membrane surface increase faster than power is increased with each additional module.

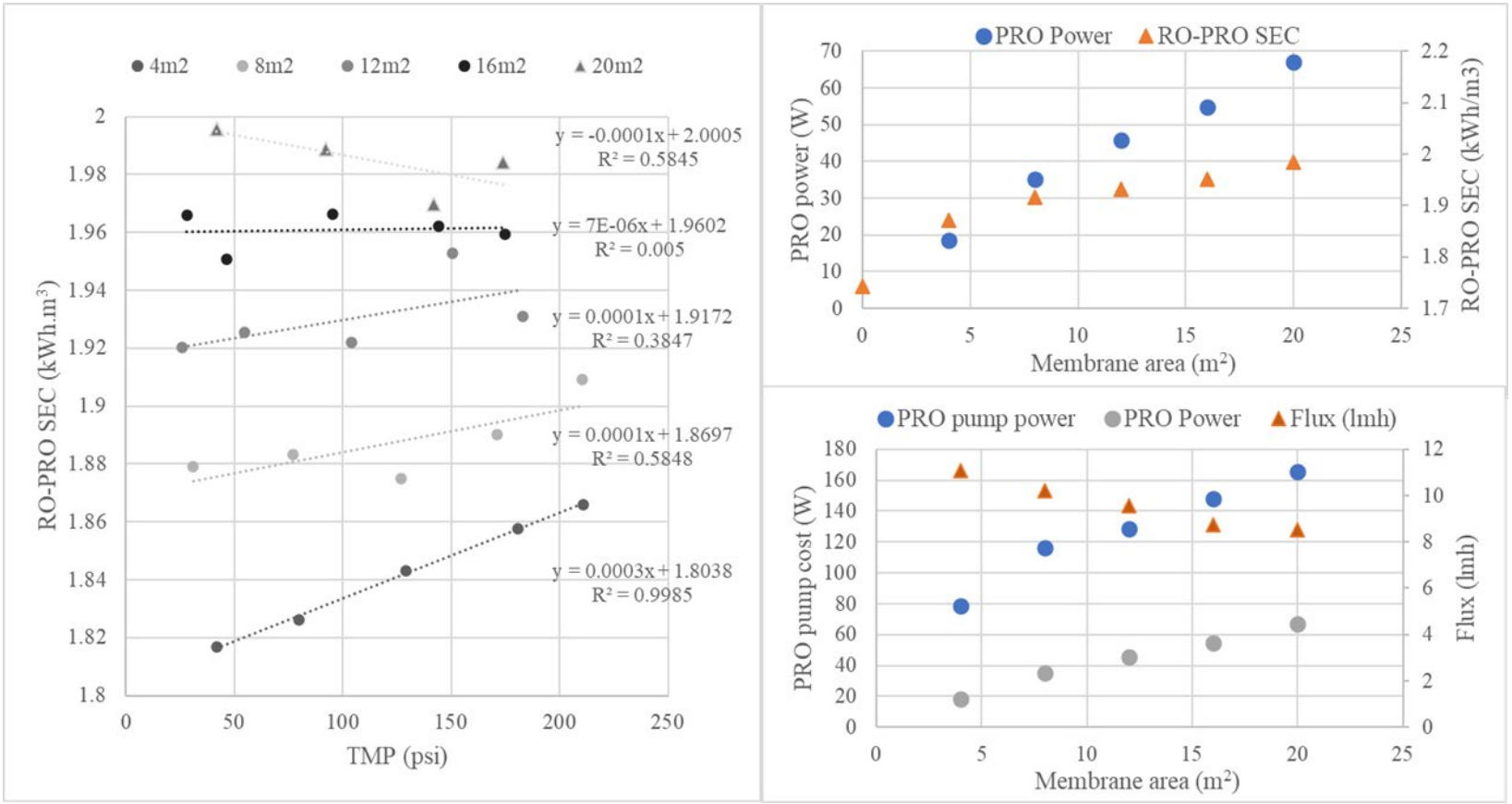

Figure 12: As additional PRO modules are added in series, the total membrane area increases in increments of 4 m^2—the membrane area per module. In general PRO power increases due to increased permeate as membrane area increases, see graph in upper right. However, the flux (permeate per membrane area) decreases as membrane area increases, as can be seen in the lower right graph. The left-side graph displays the RO-PRO total system's specific energy consumption, normalized to RO permeate (SEC), as a function of both PRO TMP and membrane area. RO-PRO SEC increases as PRO TMP and membrane area increase.

4. PRO module configurations testing draw and feed flow rate: series and parallel

Increasing PRO feed flow rates causes flux and PRO power to both increase in all series and parallel configurations (bottom two graphs in Figure 13). As draw flow rate decreases, so does flux, PRO power, and friction losses, as represented by comparing squares (draw in series, higher flow rate) to circles, draw in parallel, lower flow rate). However, the upper two graphs in Figure 13 display much higher increases in pumping power and $SEC_{RO\text{-}PRO\text{-}PX}$, compared to modest increases in power produced by the increase in PRO flux. As PRO feed rate is increased, small increases in PRO power are produced (~30W) compared to high increases in friction losses, represented by 40-80W increase in pumping power (upper right Figure 13). The configuration with both draw and feed in parallel (2:2) results in lower PRO power, lower flux, yet much lower $SEC_{RO\text{-}PRO\text{-}PX}$ and lower friction losses as represented by PRO pumping power (Figure 13). Pumping power (friction losses) are more sensitive to increased feed flow rate in the series configuration than the 2:2 parallel configuration (upper right Figure 13). The key finding from varying configuration and feed flow rate is that low flow rates are necessary to keep friction losses and parasitic loads (PRO pumping power) to a minimum.

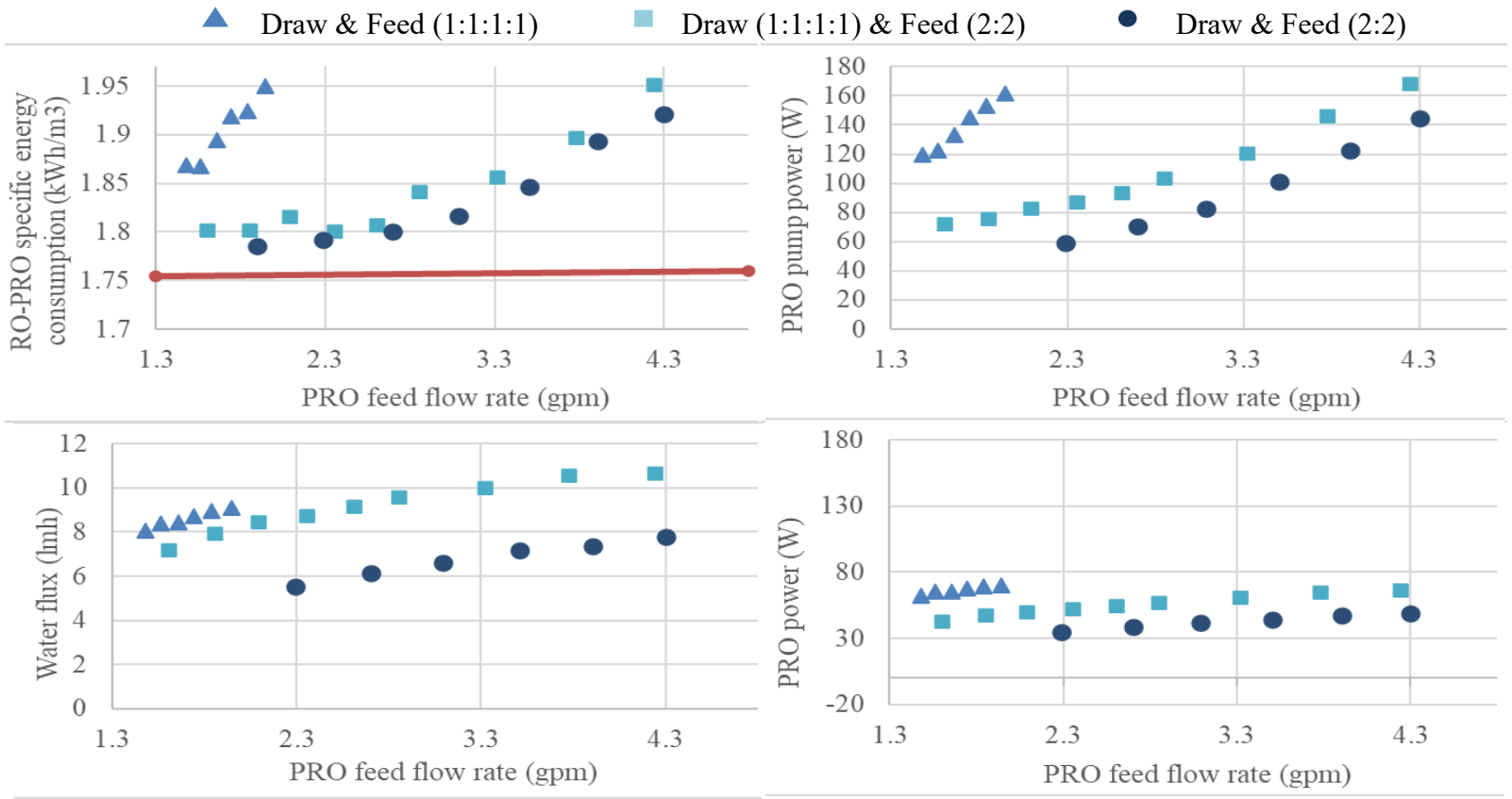

Figure 13: Operating draw and feed solutions in series results in higher friction losses (upper left and upper right), but also higher PRO flux (lmh) and PRO power produced (lower left and lower right, respectively). In series, lower feed flow rates were used because high friction losses in the feed channel caused high initial feed pressures. For all scenarios, TMP is held constant at approximately 160-180 psi. The highest flux is achieved with draw in series and feed in parallel. However, friction losses were also higher, as evidenced by higher PRO pump power.

Draw flow rate was varied with other variables held constant by adjusting the RO feed rate to produce a range of draw brine flow rates. (Figure 14). Figure 14 displays the tradeoff between increased flux and increased friction losses that result from increasing the draw flow rate—as PRO draw flow rate increases, flux increases, friction losses increase, and net power remains constant in the PRO system. This flat response of PRO power to draw flow rate indicates that friction losses are too high in the modules. There exists a value for draw flow rate below which flux diminishes sharply due to insufficient flushing of draw water across the membrane surface. The flat response across this range of draw flow rates suggests that these flow rates all provide sufficient flushing in the draw channel. However, the rate of increase in pump power required in Figure 14 is caused by friction losses in the draw channel of the PRO modules being higher than ideal. A membrane spacer in the module designed for PRO-specific flow rates could significantly reduce PRO pumping power and possibly allow for increases in flux and PRO net power across this range of draw flow rates.

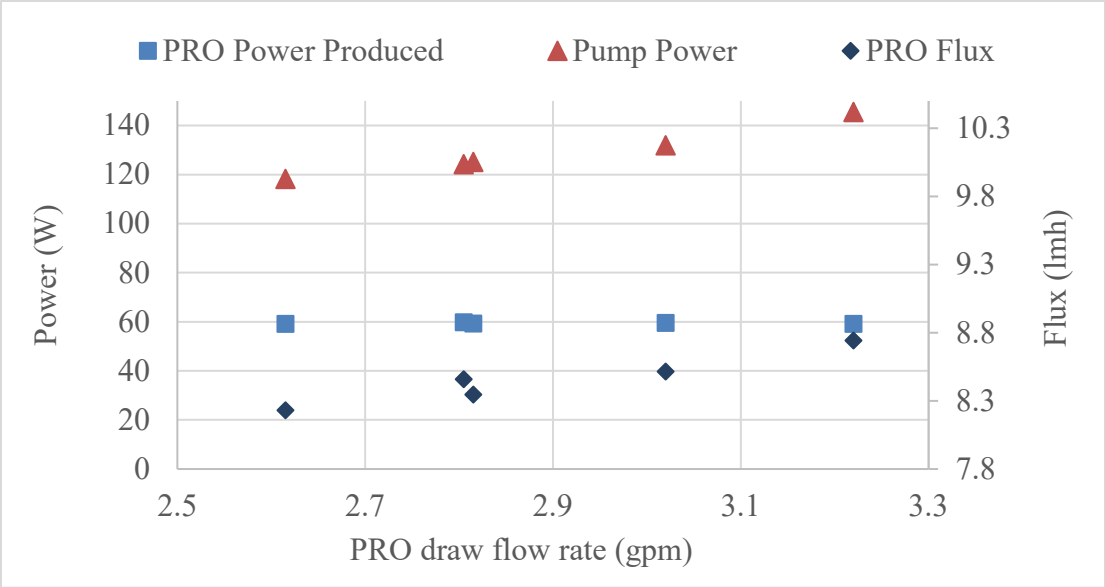

Figure 14: Potential energy recovered by the PRO system (represented by "PRO Power Produced") is approximately constant as PRO draw flow rate is increased. The increase in power gained from increasing flux is offset by increases in friction losses through the system. This test was performed with 4 modules in series, but the flux—friction tradeoff is expected to be approximately equal across the operating scenarios explored in this study.

5. Best operating point (BOP) and lowest SEC

The best operating point (BOP) for a seawater RO desalination system would be at the lowest energy consumption point for producing freshwater. The best-performing operation strategy from the tests displayed in sections 1-4 of the Results were used to test the system across the full range of RO recovery and TMP. These results are displayed in Figure 15, Figure 16, and the table of data is located in Appendix C.

Reducing pumping power and parasitic loads from friction losses constitute the first target for reductions to achieve a BOP for this pilot system. PRO pumping power is much lower than pumping power required for RO (Figure 15) because of lower operating

pressures in the PRO system. PRO power ranges from 1/3 to 1/10 the amount necessary for RO depending on RO recovery rate and PRO TMP (Figure 15). Minimizing PRO pumping requirements is necessary as these are entirely parasitic loads. The second target, and primary means to reduce pumping power is achieved by generating pressurized flow through the PRO membrane that can offset pumping needs for RO. Figure 16 displays results for $SEC_{RO\text{-}PRO\text{-}PX}$ at various values of TMP with the system set with draw and feed in 2:2 parallel configuration at 10%, 20%, 30%, and 40% RO recovery. These results include losses from system friction losses—recovery is so low at 10%, that system friction losses exceed the benefits made by lower operating pressure. Low RO recovery may result in more efficient production of freshwater, but most RO facilities operate between 40-50% recovery due to capital and maintenance costs.

The goal is to produce maximum values of PRO draw pressure and permeate flow rate crossing the PRO membrane to provide potential energy that can directly be transferred to the RO feed stream to reduce the $SEC_{RO\text{-}PRO\text{-}PX}$ (Figure 6). The lowest $SEC_{RO\text{-}PRO\text{-}PX}$ for this system can be identified by varying the TMP and RO recovery (Figure 16) after optimizing system configuration and feed and draw flow rates (Figure 13). As previously stated, the PRO draw pressure can reach approximately ½ of the osmotic pressure in the RO brine. At 40% recovery, ½ of the average osmotic pressure through the PRO draw modules was calculated to be 288 psi, more than double the achievable pressure by the Oasys membranes whose best performance is displayed at ~130 psi in Figure 16. The pilot system was unable to operate close to the theoretical optimum pressure, causing significant reductions to the amount of energy PRO could

recover from the RO brine discharge. In addition, flux rates were heavily reduced by increasing TMP in the PRO system (Figure 12), causing both lower exiting PRO draw flow rate and draw pressure than expected.

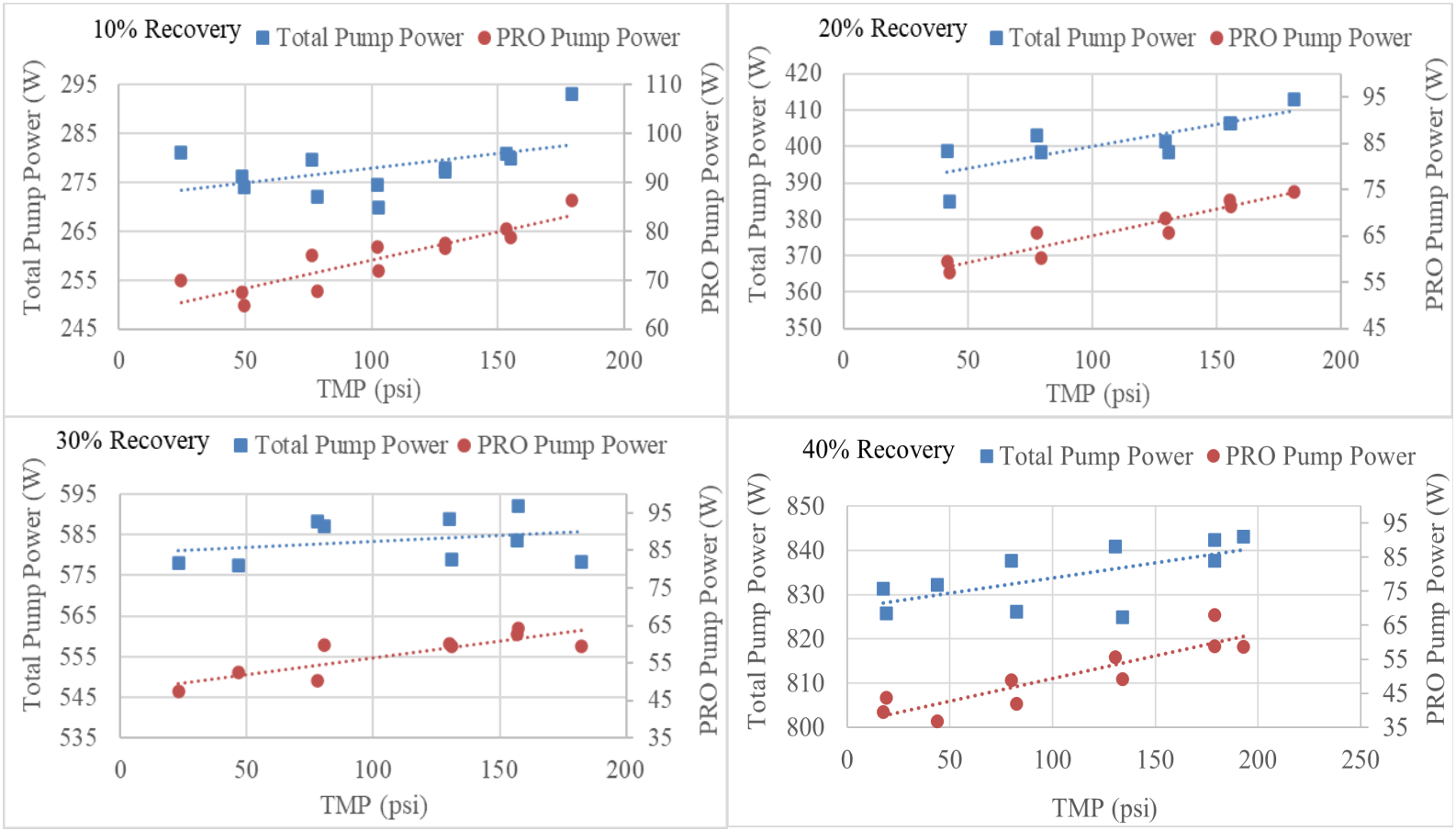

Figure 15: Total pump power (left axis) and PRO draw and feed pump power (right axis) are displayed as functions of TMP. All are linear relationships where power increases as TMP increases. With three PRO modules operated in series, the total pump power remains approximately constant with increasing TMP. The proportion of power required by each pump shifts as PRO pressure increases and exiting PRO draw flow decreases (refer to Figure 2 to place pumps in the system).

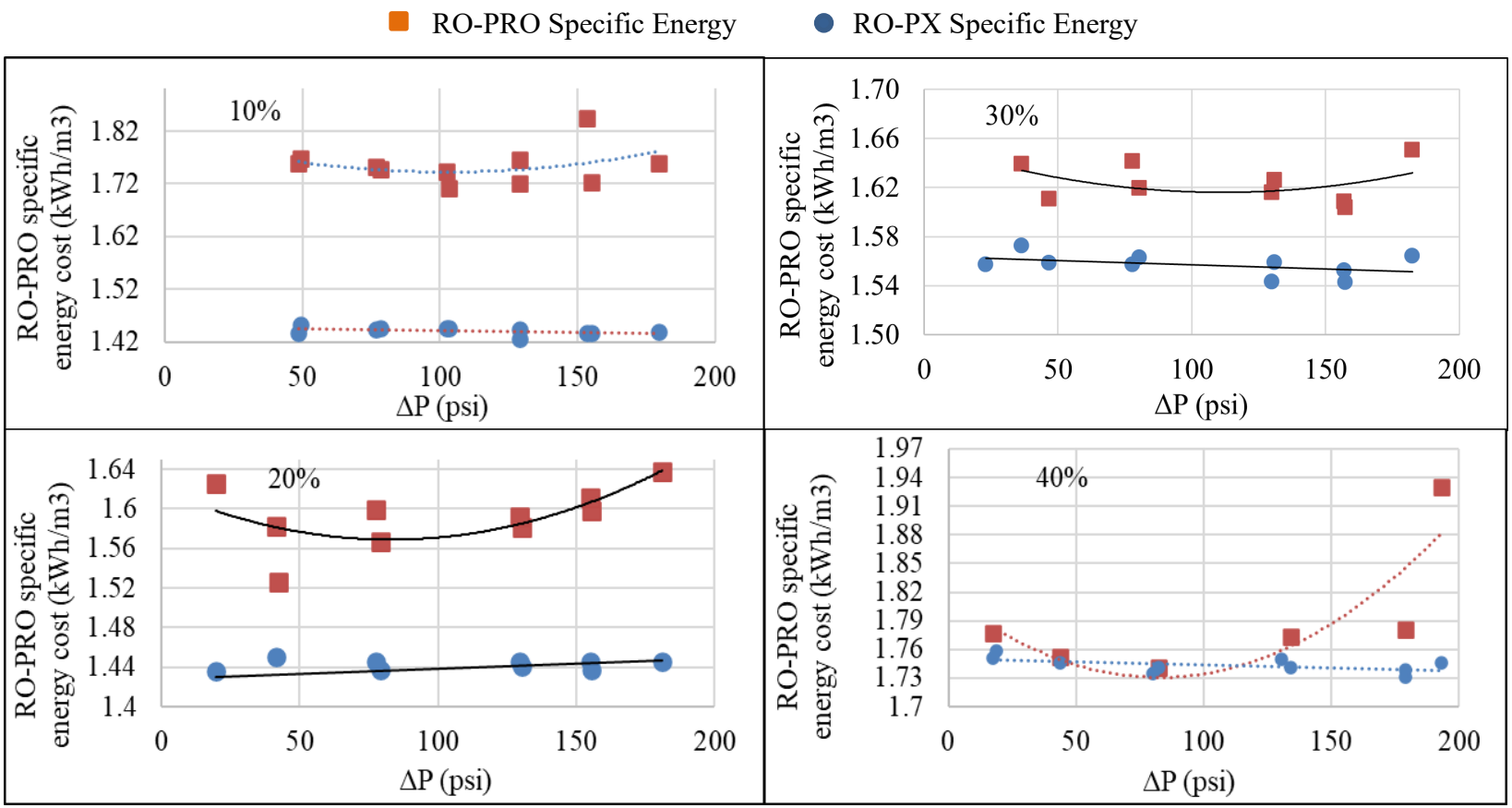

Figure 16: Four graphs depict RO-PRO combined specific energy as a function of average ΔP in the PRO system for RO recovery rates 10%, 20%, 30%, and 40%. These four RO recovery rates provide four variations for salinity in the draw solution and draw flow rate in the PRO system. Specific energy appears to be lowest at 20% recovery. This is to be expected, as specific energy in an ideal RO-PX system will be minimized at lower RO yields because freshwater is produced at a lower RO operating pressure, and energy in the exiting brine is recycled to incoming brine with the PX devices. The PRO system operates more efficiently at higher RO recoveries, as shown in lower right.

6. Impact of PRO membrane performance improvements

In Figure 16, the lower right graph shows that RO-PRO performance at 40% recovery comes close to reducing the overall specific energy cost of producing freshwater from seawater, but friction losses exceed the potential energy gained by PRO. The Oasys forward osmosis membrane modules used in this experiment were not designed specifically for operating in PRO energy production, and the feed and draw spacers could be improved based on design flow rates displayed in this study. The membrane itself, and the thin foam structural support layer for the membrane are also not designed with PRO in mind.

Current technology, based on data from previous tests (Saito et al. 2012, Wan and Ching 2015, Chen et al. 2016), provides the possibility of improving membrane performance by 2-5 times better than the tests at Samoa, CA. If currently available technology was assembled in one project, flux rates through PRO membranes could easily be doubled, friction losses through membrane spacers could be reduced by up to 50%, and improved circulation of feed and draw fluids across the membrane surface could increase the trans-membrane salinity gradient—thereby yielding a higher practical TMP and better flux rates. If solely the membrane flux was doubled, the energy recovered by PRO would exceed energy costs at 40% RO recovery and produce a 6.5% energy reduction over a standard Seawater RO system with PCX devices (Figure 17).

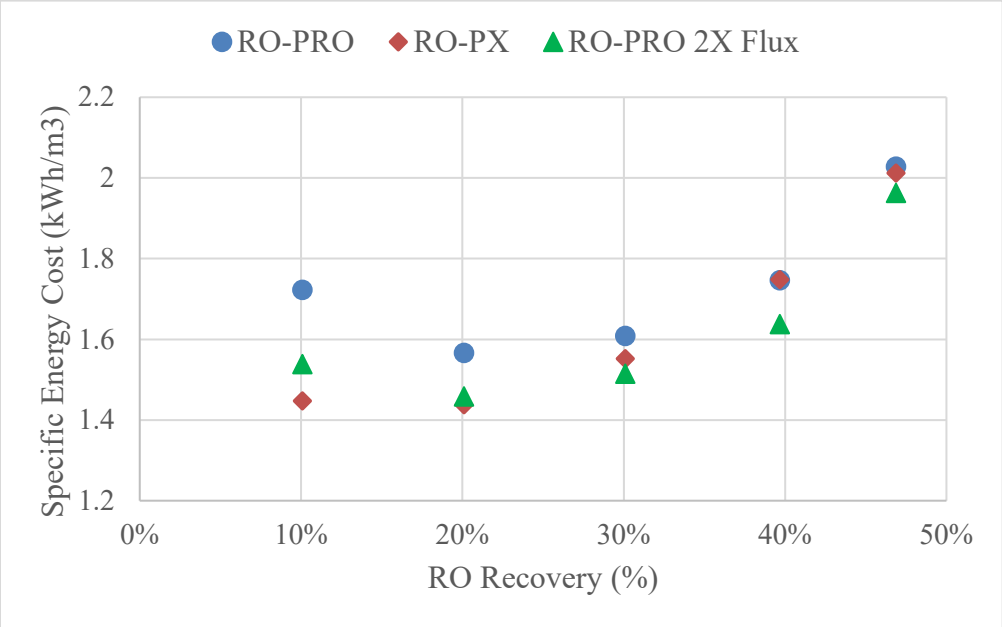

Figure 17: Specific Energy Costs are displayed for 3 scenarios scenarios—RO-PRO, RO-PX, and hypothetical RO-PRO with 2 times greater membrane flux—at the following RO recoveries: 10%, 20%, 30%, 40%, and 47%. If flux through the PRO membrane were 2X greater than measured in the pilot, total RO-PRO energy cost would fall below typical RO-PX energy cost at 30%, 40%, and 47% RO recoveries.

If PRO pressure were able to increase to closer to the osmotic pressure and maintain the same flux, then PRO power could increase and RO-PRO SEC could decrease, as displayed in Table 4. However, the improvement to system energy consumption (SEC) is slight, ranging from 0.4% to 4.7% improvement on the best operating point at each RO recovery rate. The lack of improvement, despite significant increases to PRO power (see Table 4) is due to two reasons. First, the RO-PRO SEC is dominated by pumping costs for the RO and PRO systems, which do not change as much when PRO flux (permeate) are low.

Table 4: Potential increase in PRO power and reduction in RO-PRO SEC are calculated using draw pressures midway between experimentally tested peak values and the theoretical maximum at ½ the osmotic pressure of the average salinity of the draw solution. Measured data is used for all other inputs.

TMP at peak PRO Net power (psi)	1/2 Osmotic pressure of draw solution (psi)	50% closer to osmotic pressure (psi)	% increase in PRO Power	% reduction in RO-PRO SEC
100	200	150	90%	3.1%
76	222	149	90%	4.7%
128	252	190	20%	0.4%
132	288	210	55%	2.2%
130	319	224	65%	1.1%

The second reason for the minimal improvement to SEC is that the Oasys membranes did not perform well under pressure, causing flux rates to drop very quickly as draw pressure (TMP) increased. An RO-PRO system may perform much better if the membranes were designed for PRO, and able to maintain a high osmotic gradient across the membrane at higher pressures, resulting in higher flux and elevated operating pressures. For example, other pilot tests achieved much higher flux rates at elevated pressure, such as the Mega-ton Project in Japan (Sakai et al., 2016) using hollow fiber modules.

7. Error analysis for best operating point (BOP) values

A. Measurement and device error

Precision of instruments and accuracy of measurements both combine to introduce uncertainty in the results and key findings for a BOP of the RO-PRO system. Error introduced by instrument precision is presented as “Manufacturer error range” in Table 5. Measurement error is presented as “Resolution” in Table 5, and the combined

total error range is estimated in the far right column. In calculating the BOP, only pressure and flow readings were used for RO and PRO inlets and outlets, as shown previously in Figure 6. Potential error in conductivity measurement is also presented because conductivity readings were used to determine the potential energy lost to salt diffusion through the RO and PRO membranes. Compared to pressure losses, salt diffusion provided negligible loss of potential energy, and is not reported directly in this study.

Table 5: An estimated error range is displayed for each pressure gage, flow meter, and the conductivity probe used in collecting measurement for each experiment. Estimated error range is calculated as the sum of instrument error and user measurement error, labeled as device "resolution" here. For digital flow meter and conductivity probe, resolution is precise, while for analog pressure gages, resolution is somewhat subjective.

Instrument	Resolution	Measured Range	Manufacturer error range	Total error range
RO inlet pressure gage (PG)	4 psi	350 - 850 psi	+/- 2%	+/- 3%
RO brine outlet PG	4 psi	330 - 830 psi	+/- 2%	+/- 3%
PRO draw inlet PG	2 psi	40 - 250 psi	+/- 2%	+/- 4.5%
PRO draw outlet PG	2 psi	40 - 240 psi	+/- 2%	+/- 4.5%
PRO feed inlet PG	1 psi	20 - 80 psi	+/- 2%	+/- 7%
PRO feed discharge PG	1 psi	10 - 70 psi	+/- 2%	+/- 7%
RO inlet pressure IFM SM6004 flow meter (FM)	0.01 gpm	4 - 5.5 gpm	+/- 2.5%	+/- 3%
RO permeate FM	0.01 gpm	0.5 - 2.5 gpm	+/- 2.5%	+/- 3%
PRO draw inlet FM	0.01 gpm	2.5 - 5 gpm	+/- 2.5%	+/- 3%
PRO draw outlet FM	0.01 gpm	2.5 - 5.5 gpm	+/- 2.5%	+/- 3%
PRO feed inlet FM	0.01 gpm	1.5 - 4.5 gpm	+/- 2.5%	+/- 3%
PRO feed discharge FM	0.01 gpm	1.5 - 4.5 gpm	+/- 2.5%	+/- 3%
YSI Pro 30 Conductivity probe	0.1 mS/cm	28 - 70 mS/cm	+/- 1%	+/- 1.3%

B. Propagation of potential error to Best Operating Point findings

Minimum and maximum potential error was calculated and reported in Table 6 for the BOP at each RO recovery rate (Figure 16). The measured RO and PRO pressures and flow rates for each point in the system were perturbed by the maximum potential error increase (+) or decrease (-) from Table 5. The calculated SEC with the max/min error values is presented in the fourth column of Table 6, and the values reflect significant sensitivity to measurement error. These results are most sensitive to PRO permeate flow rate, as measured by the difference between Feed inlet and outlet, averaged with the difference between Draw outlet and inlet. Even though the total potential error is only +/- 3% (Table 5), the total permeate values (ranging from 0.47 – 0.74 gpm) are low compared to the Draw and Feed flow values (ranging from 1.9 – 5.0 gpm), causing final error to increase by a factor of 3 to 10. This sensitivity to PRO permeate flow rate can be seen in the percent change of calculated RO-PRO SEC in the rightmost column Table 6. Upper and lower bracket values for RO-PRO SEC are also above and below the RO-PX SEC values (seawater RO desalination without PRO). There are values within the error bars where RO-PRO SEC is significantly below that of RO alone. However, the practice of measuring PRO permeate as both the difference between draw and feed inlets and outlets adds confidence to the findings, and the probability is very low that real values would be close to the upper or lower brackets for RO-PRO SEC shown in Table 6.

Table 6: Maximum error is displayed for upper and lower values of RO-PRO SEC. Maximum upper and lower brackets were based on perturbing the measured pressures and flow rates used in the RO-PRO SEC calculation by the maximum and minimum error values for each measurement, as estimated in.

Experiment at BOP	**RO-PX SEC (kWh/m^3)**	**Error adjustment**	**RO-PRO SEC (kWh/m^3)**	**% Change in RO-PRO SEC**
10% Recovery		Max lower bracket	1.22	-28.9%
	1.45	Measured	1.71	0.0%
		Max upper bracket	2.21	29.3%
20% Recovery		Max lower bracket	1.22	-22.1%
	1.44	Measured	1.57	0.0%
		Max upper bracket	1.91	22.2%
30% Recovery		Max lower bracket	1.34	-18.9%
	1.56	Measured	1.65	0.0%
		Max upper bracket	1.96	18.9%
40% Recovery		Max lower bracket	1.52	-14.3%
	1.74	Measured	1.77	0.0%
		Max upper bracket	2.03	14.3%
50% Recovery		Max lower bracket	1.82	-10.3%
	2.01	Measured	2.03	0.0%
		Max upper bracket	2.24	10.3%

VI. CONCLUSIONS

1. Findings

One measurement point at 40% recovery achieved lower RO-PRO SEC than the RO-PX system, using measured data and modeled system configuration and pump efficiencies. This point, however, was transient, and overall, flux rates at elevated pressures were too low to yield definitive results. The variables which dominated the final specific energy consumption were PRO flux rates, the dependence of PRO flux rates on pressure (PRO TMP), and friction losses in the membrane modules. Future efforts should focus on reducing friction losses in the modules and increasing flux rates as transmembrane pressure increases.

2. Next step for optimization

One method of optimization is to minimize or maximize a specific variable using a system of equations for a set of unknown operating parameters. The relationships between $SEC_{RO\text{-}PRO\text{-}PX}$ and the variables in Table 2 that have been explored in this effort could be fit with regression functions and used as a set of equations to solve for these variables at minimum $SEC_{RO\text{-}PRO\text{-}PX}$. This idea for a set of RO-PRO performance equations for the tradeoffs explored in this study could facilitate more accurate modeling for net PRO power and $SEC_{RO\text{-}PRO\text{-}PX}$ in similar hybrid systems. Future work could then adjust parameters such as pump and PX efficiencies and pressure-dependent membrane flux rates to find different optimal operating points based on measured performance parameters for PRO-designed membranes. Regression functions resulting from this data

would not be recommended as a predictive tool, as overall membrane performance produced lower flux at comparable pressures and lower pressure tolerance than membranes used in other studies contemporary to this one (Saito et al. 2012, Wan and Ching, 2015, Chen et al. 2016, Sakai et al. 2016). Repeating these net power-focused experiments with higher-performing membranes could yield a set of useful predictive equations. The key finding of this study is not that membrane performance needs to be improved, but rather that the targets for PRO-specific membrane improvements are increased tolerance to higher pressures, better flux rates, and improved membrane spacers for PRO applications.

REFERENCES

Achilli, Andrea, Jeri L. Prante, Nathan T. Hancock, Eric B. Maxwell, and Amy E. Childress. (2014) "Experimental Results from RO-PRO: A next Generation System for Low-Energy Desalination." Environmental Science and Technology 48(MAY): 6437–43.

Achilli, Andrea, Tzahi Y. Cath, and Amy E. Childress. (2009) "Power Generation with Pressure Retarded Osmosis: An Experimental and Theoretical Investigation." Journal of Membrane Science 343(1-2): 42–52.

Altaee, Ali, and Adel Sharif. (2015) "Pressure Retarded Osmosis: Advancement in the Process Applications for Power Generation and Desalination." Desalination 356: 31–46.

Andrews, William T., and David S. Laker. (2001) "A Twelve-Year History of Large Scale Application of Work-Exchanger Energy Recovery Technology." Desalination 138(1-3): 201–6.

Authority, S. D. C. W. (2017). "Seawater Desalination: The Claude "Bud" Lewis Desalination Plant and Related Facilities."

Cath, Tzahi Y.; Hancock, Nathan T.; Lundin, Carl D.; Hoppe-Jones, Christiane; Drewes, Jörg E. (2010) "A Multi-Barrier Osmotic Dilution Process for Simultaneous Desalination and Purification of Impaired Water." Journal of Membrane Science 362(1-2): 417–26.

Chen, Y., Setiawan, L., Chou, S., Hu, X., & Wang, R. (2016). Identification of safe and stable operation conditions for pressure retarded osmosis with high performance hollow fiber membrane. Journal of Membrane Science, 503, 90-100. doi:10.1016/j.memsci.2015.12.041

Chong, Tzyy Haur, Siew-Leng Loo, Anthony G Fane, and William B Krantz. (2015) "Energy-Efficient Reverse Osmosis Desalination: Effect of Retentate Recycle and Pump and Energy Recovery Device Efficiencies." Desalination 366: 15–31.

Feinberg, Benjamin J, Guy Z Ramon, and Eric M V Hoek. (2013) "Thermodynamic Analysis of Osmotic Energy Recovery at a Reverse Osmosis Desalination Plant." Environmental science & technology 47: 2982–89.

Feng Wan, Chun, and Tai-Shung Chung. (2015) "Osmotic Power Generation by Pressure

Retarded Osmosis Using Seawater Brine as the Draw Solution and Wastewater Retentate as the Feed." Journal of Membrane Science 479: 148–58.

Fritzmann, C., J. Löwenberg, T. Wintgens, and T. Melin. (2007) "State-of-the-Art of Reverse Osmosis Desalination." Desalination 216(1-3): 1–76.

Han, Gang, Sui Zhang, Xue Li, and Tai-Shung Chung. (2015) "Progress in Pressure Retarded Osmosis (PRO) Membranes for Osmotic Power Generation." Progress in Polymer Science 51: 1–27.

He, Wei, Yang Wang, Adel Sharif, and Mohammad Hasan Shaheed. (2014) "Thermodynamic Analysis of a Stand-Alone Reverse Osmosis Desalination System Powered by Pressure Retarded Osmosis." Desalination 352: 27–37.

Kim, David Inhyuk, Jungwon Kim, Ho Kyong Shon, and Seungkwan Hong. (2015) "Pressure Retarded Osmosis (PRO) for Integrating Seawater Desalination and Wastewater Reclamation: Energy Consumption and Fouling." Journal of Membrane Science 483: 34–41.

Kim, Jihye, Minkyu Park, Shane a. Snyder, and Joon Ha Kim. (2013) "Reverse Osmosis (RO) and Pressure Retarded Osmosis (PRO) Hybrid Processes: Model-Based Scenario Study." Desalination 322: 121–30.

Kim, Yu Chang Young, Yu Chang Young Kim, Dongwook Oh, and Kong Hoon Lee. (2013) "Experimental Investigation of a Spiral-Wound Pressure-Retarded Osmosis Membrane Module for Osmotic Power Generation." Environmental Science and Technology 47(6): 2966–73.

Lee, Kah Peng, Tom C. Arnot, and Davide Mattia. (2011) "A Review of Reverse Osmosis Membrane Materials for desalination—Development to Date and Future Potential." Journal of Membrane Science 370(1–2): 1–22.

Li, Ye, Rong Wang, Saren Qi, and Chuyang Tang. (2015) "Structural Stability and Mass Transfer Properties of Pressure Retarded Osmosis (PRO) Membrane under High Operating Pressures." Journal of Membrane Science 488: 143–53.

Loeb, S., and G.D. Mehta. (1979) A Two-Coefficient Water Transport Equation for Pressure-Retarded Osmosis.pdf." : 351–62.

Maisonneuve, Jonathan, Pragasen Pillay, and Claude B. Laflamme. (2015) "Pressure-Retarded Osmotic Power System Model Considering Non-Ideal Effects." Renewable Energy 75: 416-424.

Peñate, Baltasar, and Lourdes García-Rodríguez. (2012) “Current Trends and Future Prospects in the Design of Seawater Reverse Osmosis Desalination Technology.” Desalination 284: 1–8.

Prante, Jeri L., Jeffrey A. Ruskowitz, Amy E. Childress, and Andrea Achilli. (2014) “RO-PRO Desalination: An Integrated Low-Energy Approach to Seawater Desalination.” Applied Energy 120: 104–14.

Saito, Keiichiro; Irie, Morihiro; Zaitsu, Shintaro; Sakai, Hideyuki; Hayashi, Hidechito; Tanioka, Akihiko (2012) “Power Generation with Salinity Gradient by Pressure Retarded Osmosis Using Concentrated Brine from SWRO System and Treated Sewage as Pure Water.” Desalination and Water Treatment 41(1-3): 114–21.

Sakai, H., Ueyama, T., Irie, M., Matsuyama, K., Tanioka, A., Saito, K., & Kumano, A. (2016). Energy recovery by PRO in sea water desalination plant. Desalination, 389, 52-57. doi:10.1016/j.desal.2016.01.025

Sauvet-Goichon, Bruno. (2007) “Ashkelon Desalination Plant - A Successful Challenge.” Desalination 203(1-3): 75–81.

Shenvi, Seema S., Arun M. Isloor, and A.F. Ismail. (2015) “A Review on RO Membrane Technology: Developments and Challenges.” Desalination 368: 10–26.

Shrivastava, Abhishek, Steven Rosenberg, and Martin Peery. (2015) “Energy Efficiency Breakdown of Reverse Osmosis and Its Implications on Future Innovation Roadmap for Desalination.” Desalination 368: 181–92.

Shumway, S. A. (1999) “The Work Exchanger for SWRO Energy Recovery.” International Desalination and Water Reuse Quarterly 8(4): 27–33.

Sim, Victor S.; She, Q.; Chong, T. H.; Tang, C. Y.; Fane, A. G.; Krantz, W. B. (2013) “Strategic Co-Location in a Hybrid Process Involving Desalination and Pressure Retarded Osmosis (PRO).” Membranes 3(3): 98–125.

Skilhagen, Stein Erik, Jon E. Dugstad, and Rolf Jarle Aaberg. (2008) “Osmotic Power - Power Production Based on the Osmotic Pressure Difference between Waters with Varying Salt Gradients.” Desalination 220(1-3): 476–82.

Skilhagen, S. E. (2010). Osmotic power — a new, renewable energy source. *Desalination and Water Treatment*, 271-278.

Stover, Richard L., and Bill Andrews. (2012) “Isobaric Energy-Recovery Devices: Past, Present, and Future.” IDA Journal of Desalination and Water Reuse 4(1): 38–43.

Straub, Anthony P, Chinedum O Osuji, Tzahi Y Cath, and Menachem Elimelech. (2015) "Selectivity and Mass Transfer Limitations in Pressure-Retarded Osmosis at High Concentrations and Increased Operating Pressures." Environmental science & technology 49 (20): 12551–12559

United Nations. (2015) Water for a Sustainable World. Paris, France: UNESCO. http://unesdoc.unesco.org/images/0023/002318/231823E.pdf.

Yip, Ngai Yin, and Menachem Elimelech. (2012) "Thermodynamic and Energy Efficiency Analysis of Power Generation from Natural Salinity Gradients by Pressure Retarded Osmosis." Environmental Science and Technology 46(9): 5230–39.

Zhu, Aihua, Panagiotis D. Christofides, and Yoram Cohen. (2009) "Minimization of Energy Consumption for a Two-Pass Membrane Desalination: Effect of Energy Recovery, Membrane Rejection and Retentate Recycling." Journal of Membrane Science 339(1-2): 126–37.

APPENDICES

Appendix A: Equipment pictures

Figure 18: Pretreatment system—1. blue cartridge filters for seawater pretreatment and PRO feed carbon block treatment in lower left corner, 2. ultrafiltration unit center, 3. white seawater coagulation mix tank center right, 4. large green treated

seawater storage tank upper right. 5. lower center left white bucket with coagulant/antiscalant and MixRite proportional injector (on tripod). Trailer is through doors to left.

Figure 19: Trailer that housed the RO and PRO membrane modules, testing equipment, pumps, electrical, tools, and spare parts. Picture taken prior to installation.

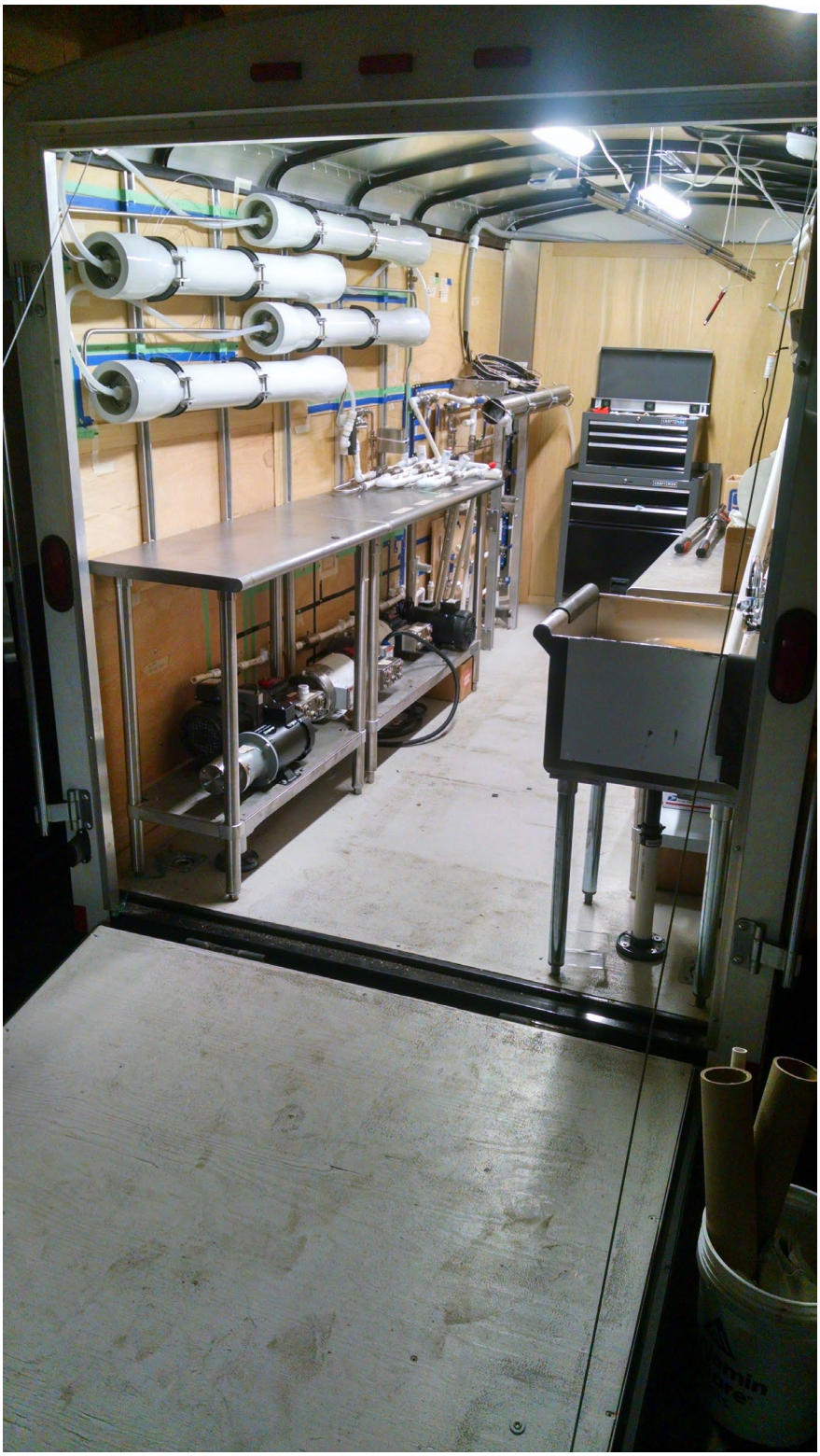

Figure 20: Overall trailer layout from rear door

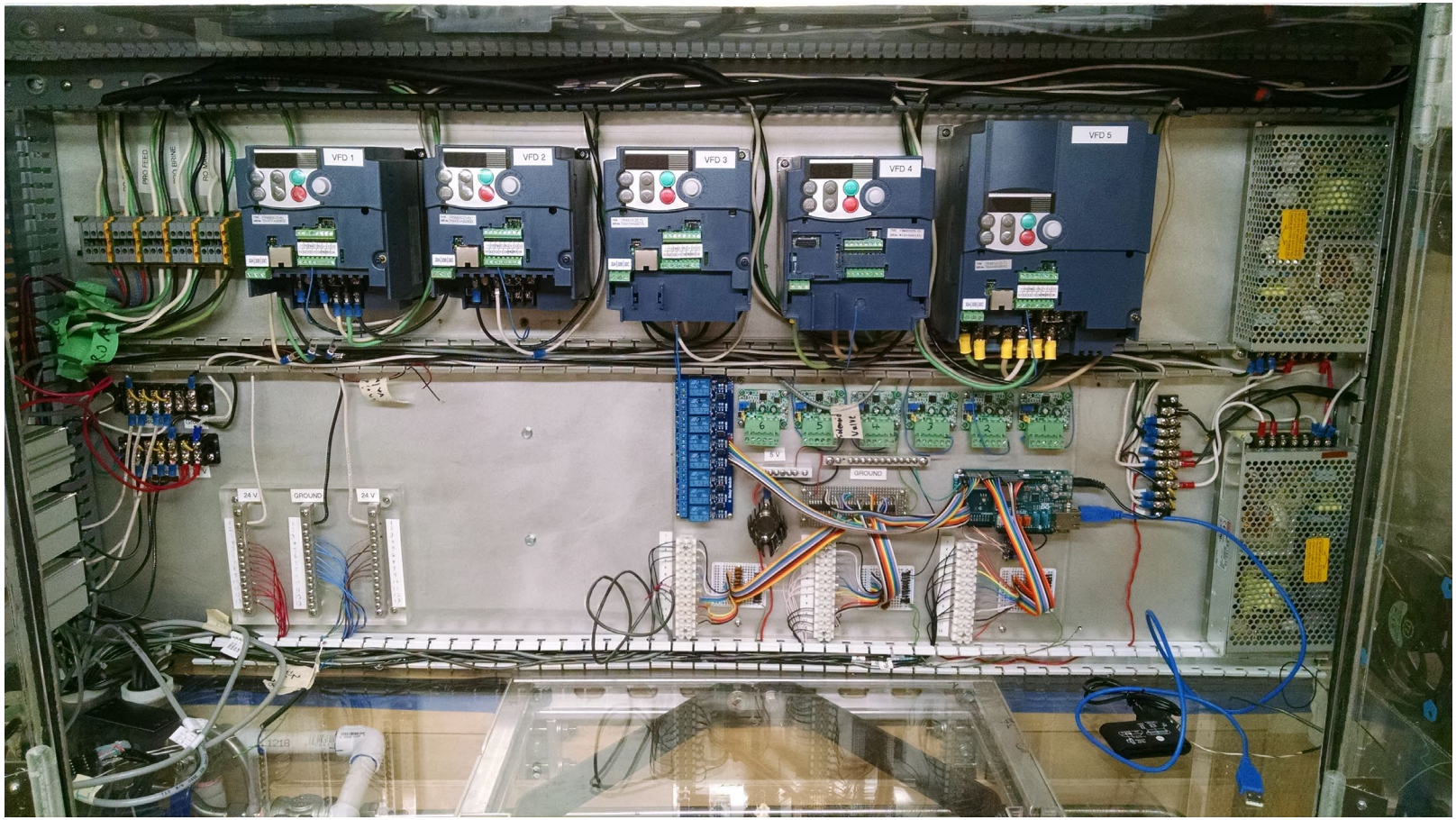

Figure 21: Electrical control panel for sensors, and control systems. Blue boxes along the top are variable frequency drives (VFDs) for powering pumps.

Figure 22: view of pipe network delivering feed and draw solution to PRO membrane modules. High-pressure draw solution is delivered in stainless steel tubing, and feed solution is delivered in clear plastic tubing.

Appendix B: Methods experimental conditions

Table 7: The number of experiments and the experimental conditions that were tested with the RO-PRO pilot are laid out in this table. In Test 4 and 5, feed flow rate was reduced slightly as TMP increased in order to maintain relatively constant feed pressure and average feed flow rates through the module.

Test	Experiment	Number of experimental data points	RO in Pressure (psi)	PRO Draw in Pressure (psi)	TMP (psi)	TMP increment (psi)	PRO Feed out Pressure (psi)	RO Feed Q (gpm)	PRO Draw Flow rate (gpm)	PRO Feed in Q (gpm)	PRO Feed increment (gpm)
1: Membrane Area (modules in series)	1 Module	10	711	56 - 230	40 - 211	~50	0 - 0.5	5.0	3.0	2.5	
	2 Modules	10	711	53 - 242	32-210	~50	0	5.0	3.0	2.5	
	3 Modules	10	711	70 - 238	33 - 201	~50	10	5.0	3.0	2.5	
	4 Modules	10	711	74 - 231	29 - 175	~50	10	5.0	3.0	2.5	
	5 Modules	10	711	91 - 240	39 - 180	~50	10	5.0	3.0	2.5	
2: Feed Flow Rate	5 modules in series	6	711	235	180	n/a	10	5.0	3.0	1.83 - 2.34	0.1
	5 modules in series	7	711	214	160	n/a	10	5.0	3.0	1.73 - 2.34	0.1
	Draw: 1:1:1:1, Feed 2:2	9	711	220 - 228	190	n/a	5	5.0	3.0	1.85 - 4.61	0.25 - 0.5
	Draw 2:2, Feed 2:2	7	711	200 - 209	178	n/a	5	5.0	3.0	2.09 - 4.56	0.4
3: Module configuration	4 in series (1:1:1:1)	10	711	74 - 231	29 - 175	~50	10	5.0	3.0	2.5	
	Draw in series (1:1:1:1), Feed in parallel (2:2)	10	711	74 - 237	22 - 207	~50	5	5.0	3.0	3.2 - 3.3	
	Draw in parallel (2:2), Feed in parallel (2:2)	9	711	55 - 209	16 - 192	~50	5	5.0	3.0	2.6 - 2.9	

Test	Experiment	Number of experimental data points	RO in Pressure (psi)	PRO Draw in Pressure (psi)	TMP (psi)	TMP increment (psi)	PRO Feed out Pressure (psi)	RO Feed Q (gpm)	PRO Draw Flow rate (gpm)	PRO Feed in Q (gpm)	PRO Feed increment (gpm)
4: Best Operating Point: Lowest SEC for RO-PRO seawater desalination	10% RO Recovery	11	433	90 - 199	22 -178	~25	5	5.0	4.3	2.4 - 2.8	
	20% RO Recovery	10	512	77-199	16 - 180	25 - 50	5	5.0	3.9	2.4 - 2.7	
	30% RO Recovery	10	602	68 - 199	20 -181	~40	5	5.0	3.5	2.5 - 2.9	
	40% RO Recovery	9	711	55 - 209	16 - 192	~50	5	5.0	3.0	2.6 - 2.9	
	50% RO Recovery	8	841	48 - 199	15 -183	25 - 50	5	5.3	2.7	2.7 - 2.9	

Appendix C: Sample data

Table 8: Calibrated and adjusted measurements from RO-PRO pilot for BOP experiments at 10%, 20%, 30%, 40%, and 50% RO recoveries.

seawater in Pressure	P3 RO in Pressure (psi)	P4 RO out Pressure (psi)	P6 PRO in Pressure (psi)	P8 PRO out Pressure (psi)	PRO Feed in Press (psi)	PRO Feed out Press (psi)	TMP (psi)	RO Feed Q (gpm)	RO Brine Q (gpm)	RO Perm Q (gpm)	PRO Draw out Q (gpm)	PRO Feed in Q (gpm)	PRO Feed out Q (gpm)
10%													
0	433.2	413.2	95.3	77.0	70	59	21.7	5.01	4.35	0.7	5.37	2.78	1.8
0	433.2	413.2	90.2	73.0	40	30	46.6	5.01	4.35	0.69	5.21	2.72	1.89
0	433.2	413.2	95.3	78.9	18	5.0	75.6	5.02	4.35	0.7	5.04	2.63	1.97
0	433.2	413.2	120.2	103.9	18	5.0	100.6	5.02	4.365	0.69	4.93	2.57	2.04
0	433.2	413.2	147.2	130.8	19	5.0	127.0	5.02	4.35	0.71	4.81	2.52	2.1
0	433.2	413.2	173.2	158.6	20	5.0	153.4	5.01	4.345	0.7	4.7	2.46	2.14
0	433.2	413.2	199.1	183.6	21	5.0	178.3	5.02	4.355	0.7	4.6	2.41	2.2
0	433.2	413.2	172.1	156.7	20	5.0	151.9	5	4.335	0.7	4.7	2.47	2.14
0	433.2	413.2	147.2	131.7	20	5.0	127.0	5.01	4.34	0.7	4.79	2.51	2.09
0	433.2	413.2	121.3	103.9	20	5.0	100.1	5.01	4.355	0.69	4.92	2.57	2.04
0	433.2	413.2	95.3	76.0	19	5.0	73.7	5.01	4.34	0.7	5.01	2.62	1.98
0	433.2	413.2	90.2	73.0	42	30	45.6	5.01	4.345	0.7	5.16	2.7	1.92
20%													
0	512.8	492.8	85.0	69.0	71	50	16.5	5.01	3.935	1.11	5.01	3.83	2.79
0	512.8	492.8	77.7	62.0	36	25	39.4	5.01	3.975	1.11	4.79	2.73	1.99
0	512.8	492.8	95.3	80.9	18.5	5.0	76.4	5.01	3.92	1.12	4.61	2.69	2.03
0	512.8	492.8	147.2	134.7	20	5.0	128.5	5.01	3.93	1.11	4.39	2.52	2.09

seawater in Pressure	P3 RO in Pressure (psi)	P4 RO out Pressure (psi)	P6 PRO in Pressure (psi)	P8 PRO out Pressure (psi)	PRO Feed in Press (psi)	PRO Feed out Press (psi)	TMP (psi)	RO Feed Q (gpm)	RO Brine Q (gpm)	RO Perm Q (gpm)	PRO Draw out Q (gpm)	PRO Feed in Q (gpm)	PRO Feed out Q (gpm)
0	512.8	492.8	173.2	159.6	20	5.0	153.9	5.01	3.92	1.12	4.31	2.48	2.12
0	512.8	492.8	199.1	186.5	21	5.0	179.8	5.01	3.925	1.11	4.21	2.43	2.17
0	512.8	492.8	173.2	159.6	21	5.0	153.4	5.01	3.925	1.11	4.32	2.5	2.13
0	512.8	492.8	147.2	133.7	21	5.0	127.5	5.01	3.925	1.11	4.41	2.53	2.07
0	512.8	492.8	95.3	78.9	20	5.0	74.6	5.01	3.925	1.11	4.62	2.64	1.97
0	512.8	492.8	77.7	62.0	38	25	38.4	5.01	3.92	1.11	4.78	2.72	1.88
30%													
0	602.4	582.4	77.7	64.0	56	46	34.2	5.07	3.51	1.58	4.68	2.9	1.75
0	601.4	581.4	72.5	59.0	27.5	17	49.1	5.07	3.505	1.58	4.5	2.8	1.82
0	602.4	582.4	95.3	81.9	17	5.0	77.4	5.07	3.515	1.57	4.32	2.75	1.96
0	602.4	582.4	147.2	133.7	18	5.0	128.5	5.07	3.495	1.59	4.04	2.56	2.03
0	602.4	582.4	173.2	163.6	20	5.0	155.9	5.06	3.505	1.59	3.97	2.51	2.08
0	602.4	582.4	199.1	188.5	20	5.0	181.1	5.06	3.49	1.58	3.85	2.47	2.12
0	602.4	582.4	173.2	163.6	20	5.0	155.6	5.06	3.505	1.58	3.98	2.53	2.08
0	602.4	582.4	147.2	133.7	20	5.0	128.2	5.07	3.515	1.59	4.07	2.56	2.04
0	602.4	582.4	95.3	78.9	19	5.0	67.1	5.07	3.51	1.58	4.28	2.72	1.97
0	602.4	582.4	68.4	54.0	34	22	47.2	5.06	3.48	1.58	4.47	2.81	1.82
40%													
0	710.9	690.9	61.1	49.1	46	36	29.3	5.08	3.03	2.08	4.25	2.9	1.7
0	710.9	690.9	55.9	46.1	16	5.0	40.2	5.08	3.02	2.07	4.1	2.82	1.77
0	710.9	690.9	95.3	85.9	17	5.0	79.4	5.08	3.015	2.08	3.94	2.75	1.85
0	711.9	691.9	148.3	138.7	18	5.0	129.2	5.08	3.025	2.08	3.75	2.65	1.93

seawater in Pressure	P3 RO in Pressure (psi)	P4 RO out Pressure (psi)	P6 PRO in Pressure (psi)	P8 PRO out Pressure (psi)	PRO Feed in Press (psi)	PRO Feed out Press (psi)	TMP (psi)	RO Feed Q (gpm)	RO Brine Q (gpm)	RO Perm Q (gpm)	PRO Draw out Q (gpm)	PRO Feed in Q (gpm)	PRO Feed out Q (gpm)
0	711.9	691.9	199.1	190.5	29	5.0	179.8	5.08	3.025	2.08	3.59	2.57	2.03
0	711.9	691.9	209.5	200.5	21	5.0	184.6	5.08	3.05	2.07	3.41	2.48	2.11
0	711.9	691.9	209.5	200.5	50.5	5.2	178.8	5.08	3.03	2.07	3.61	4.56	4.04
0	711.9	691.9	95.3	83.9	20	5.0	55.9	5.09	3.05	2.05	3.82	2.71	1.93
0	711.9	691.9	77.7	64.0	60	50	43.4	5.09	0	2.06	4.18	2.81	1.7
50%													
0	841.3	821.3	48.7	39.1	35	23	14.9	5.31	2.7	2.63	3.79	2.93	1.86
0	841.3	821.3	69.4	59.0	19	5.0	52.2	5.3	2.73	2.61	3.6	2.84	2.01
0	841.3	821.3	95.3	83.9	20	5.0	77.1	5.31	2.695	2.61	3.44	2.79	2.04
0	841.3	821.3	147.2	138.7	20	5.0	130.5	5.31	2.71	2.61	3.27	2.68	2.13
0	841.3	821.3	199.1	193.5	22	5.0	182.8	5.32	2.71	2.62	3.1	2.62	2.24
0	841.3	821.3	147.2	138.7	22	5.0	129.5	5.31	2.7	2.62	3.27	2.75	2.19
0	841.3	821.3	95.3	85.9	20	5.0	78.1	5.32	2.72	2.62	3.47	2.79	2.06
0	841.3	821.3	48.7	39.1	33	20	17.4	5.33	2.735	2.61	3.76	2.91	1.9

Table 9: Specific energy consumption, PRO power, and power density for BOP experiments at 10%, 20%, 30%, 40%, and 50% RO recoveries.

Total Pump SEC (kWh/m^3)	RO-PX SEC (kWh/m^3)	PRO Gross Power (W)	Power Density (W/m^2)	Total Pump SEC (kWh/m^3)	RO-PX SEC (kWh/m^3)	PRO Gross Power (W)	Power Density (W/m^2)
10% Recovery				30% Recovery			
1.77	1.43	34.15	2.13	1.59	1.56	32.58	2.04
1.75	1.45	27.3	1.71	1.61	1.56	25.55	1.60
1.71	1.45	23.7	1.48	1.62	1.56	28.69	1.79
1.72	1.45	25.53	1.60	1.63	1.56	31.71	1.98
1.72	1.43	26.16	1.64	1.60	1.54	33.10	2.07
1.76	1.44	24.5	1.53	1.65	1.56	29.52	1.85
1.84	1.44	19.56	1.22	1.61	1.55	33.81	2.11
1.77	1.44	24.87	1.55	1.62	1.54	32.29	2.02
1.74	1.44	25.79	1.61	1.64	1.56	26.44	1.65
1.75	1.45	25.53	1.60	1.64	1.57	23.27	1.45
1.76	1.44	22.14	1.38	40% Recovery			
1.74	1.44	25.87	1.62	1.76	1.74	26.15	1.63
20% Recovery				1.78	1.75	21.45	1.34
1.63	1.44	24.46	1.53	1.75	1.75	34.39	2.15
1.53	1.40	21.99	1.37	1.74	1.74	44.35	2.77
1.57	1.44	24.3	1.52	1.77	1.74	46.83	2.93
1.58	1.44	26.96	1.69	1.78	1.73	33.58	2.10
1.6	1.44	27.08	1.69	1.93	1.75	48.84	3.05
1.64	1.45	23.13	1.45	1.79	1.76	28.48	1.78
1.61	1.45	27.43	1.71	3.71	3.96	31.46	1.97
1.59	1.45	28.22	1.76	50% Recovery			
1.60	1.45	23.87	1.49	2.03	2.00	18.54	1.16
1.58	1.45	23.2	1.45	2.02	1.99	22.34	1.40
				2.05	2.02	27.20	1.70
				2.03	2.01	33.79	2.11
				2.04	2.01	32.83	2.05
				2.03	2.01	34.40	2.15
				2.03	2.00	28.03	1.75
				2.04	2.01	17.43	1.09